



UNIVERSITY OF POTSDAM

BACHELOR THESIS

---

# **Ultrafast dynamics of azobenzene in polyelectrolyte thin films**

---

Author:

Alexander VON REPPERT

Supervisor and first assessor :

Prof. Dr. Matias BARGHEER

Second assessor :

Prof. Dr. Ralf MENZEL

Faculty of Mathematics and Science  
Institute for Physics and Astronomy  
August 8, 2012



## Abstract

We study the optical properties of azobenzene incorporated into a polyelectrolyte matrix via spin assisted layer-by-layer deposition of PAzo-PAH double layers. Steady state transmission spectroscopy shows the absorption of the dominant  $\pi\pi^*$ -transition of this system at 365 nm that can be reduced by irradiation in the UV, which indicates the photo-induced trans-cis isomerization process. Pump-probe spectroscopy with femtosecond laser pulses at  $\lambda_{\text{pump}} = 400$  nm yields an exponential decay with a time constant in the order of 5 ps for the transient absorption, which differs from the results measured on azobenzene in solution that are published in the literature. In addition a relatively constant offset in the transient absorption has been observed that decays on a second, larger time scale of approximately 60 ps. The excitation of the trans-cis isomerization of the azobenzene molecules launches a strain pulse with dominant GHz frequency components into the adjacent quartz substrate that is studied via stimulated Brillouin backscattering experiments. A comparison of the phase of the Brillouin oscillations triggered by the azobenzene-polyelectrolyte layer with those triggered by the expansion of a well characterized gold-nanoparticle-polyelectrolyte composite as well as the oscillations triggered by the expansion of a thin aluminium film is carried out to classify the behavior of azobenzene upon excitation. At this point of the investigations the collected evidence is not conclusive to decide whether azobenzene is expanding or contracting, but the further procedure has been developed. Since the amplitude of the Brillouin oscillations are found to be equally large for the azobenzene polyelectrolyte composite and the reference samples further investigation on applications of the prepared thin films as transducers is suggested.

## Kurzfassung

Wir untersuchen die optischen Eigenschaften von Azobenzen in einer Polyelektrolyt Umgebung, die mittels rotationsgestützter Schicht für Schicht-Abscheidung von PAzo-PAH Doppelschichten hergestellt wurde. Gleichgewichts Transmissionsspektroskopie zeigt die Absorption des dominanten  $\pi\pi^*$ -Übergang dieses Systems bei 365 nm, welche durch Bestrahlung im UV-Bereich mittels photoinduzierter trans-cis-Isomerisierung reduziert werden kann. Pump-Probe-Spektroskopie mit Femtosekunden-Laserpulsen bei einer zentralen Wellenlänge von  $\lambda_{\text{pump}} = 400$  nm ergab ein exponentielles Abklingen der transienten Absorption mit einer Zeitkonstante in der Größenordnung von 5 ps, die von den Werten abweicht, die für Azobenzen in Lösung in der Literatur publiziert wurden. Zusätzlich wurde ein relativ konstanter Anteil in der transienten Absorption beobachtet, der auf einer weiteren, größeren Zeitskala von etwa 60 ps abklingt. Die Anregung der trans-cis-Isomerisierung der Azobenzenmoleküle lenkt Atome aus ihrer Ruhelage aus und erzeugt somit einen Schallpuls mit dominantem GHz Frequenzanteil, der in das Quarzsubstrat propagiert und mittels Experimenten zur stimulierten Brillouin Rückstreuung untersucht wird. Ein Vergleich der Phase der gemessenen Brillouin Oszillationen, verursacht durch die angeregte dünne Azobenzen-Polyelektrolytschicht, mit denen, ausgelöst durch die Ausdehnung einer gut charakterisierten Gold-Nanopartikel-Polyelektrolyt-Komposit Probe, sowie mit den Oszillationen, ausgelöst durch die Expansion einer dünnen Aluminiumschicht, wurde durchgeführt um das Verhalten der Azobenzenmoleküle einordnen zu können. Die gesammelten Hinweise lassen noch keinen eindeutigen Schluss zu, ob Azobenzen sich nach der Anregung ausdehnt oder zusammenzieht, aber die weitere Vorgehensweise wurde entwickelt. Da die Amplitude der Brillouin Oszillationen vergleichbar groß für Azobenzen in einer Polyelektrolyt-Umgebung und den Referenzproben ist, schlagen wir weitere Untersuchungen zu möglichen Anwendungen der hergestellten dünnen Schichten als optisch-mechanische Energiewandler vor.



### Acknowledgements

Although a complete fulfillment of this task would go beyond the given framework I would like to thank all persons who have supported me on the way to this thesis. To begin with I would like to express my gratitude to my supervisor Prof. Dr. Matias Bargheer for the intense and stimulating guidance at every stage of the work. His continuous trust and openness encouraged me to perform at my best.

I am very grateful to the entire team of the Ultrafast Dynamics in Condensed Matter group for the positive and helpful atmosphere that gave me a comfortable place to work and learn from experienced Postdoc, Phd and Diploma students.

In particular I would like to mention Mareike Kiel and Steffen Mitzscherling as the pioneers of the group in the field of studying thin polyelectrolyte films with ultrafast methods. Mareike and Steffen patiently introduced me to the routines in the laser laboratory and to the sample preparation process. Steffen supported me on many measurements at the pump-probe setup and the transmission spectrometer.

Furthermore I would like to thank Daniel Schick for taking care of the good technical infrastructure of the group, for his commitment to tweak the best possible performance out of the used devices and for stylistic hints concerning the presentation of the results. I am also indebted to André Bojahr for the great computational support he gave by introducing me to MATLAB and for many inspiring and cheerful discussions. In addition I would like to thank Marc Herzog for sharing his experience and interesting discussion on possible improvements on my experiments.

Finally, but first in my heart I would like to thank my family, Levke and my friends who are a safe haven in my life. I also thank my fellow students for the fun we had in and outside the university.

Thank you all.

# Contents

<b>1</b>	<b>Introduction</b>	<b>1</b>
1.1	Structure of this thesis . . . . .	2
1.2	Motivating literature . . . . .	2
<b>2</b>	<b>Preparation and sample characterization</b>	<b>6</b>
2.1	Spin assisted layer-by-layer deposition . . . . .	6
2.2	Steady state transmission spectroscopy . . . . .	9
2.2.1	Transmission spectra of the used samples . . . . .	9
2.2.2	Reversible photoswitching in azobenzene thin films . . . . .	12
<b>3</b>	<b>Pump-probe spectroscopy</b>	<b>14</b>
3.1	Experimental setup . . . . .	14
3.2	Relative transmittance measurements . . . . .	16
3.2.1	Measurement and data analysis . . . . .	16
3.2.2	Discussion of the results . . . . .	18
3.3	Transient reflectivity measurements . . . . .	22
3.3.1	Theoretical background to the Brillouin oscillation measurements . .	22
3.3.2	Measurement and signal analysis of reflectivity change . . . . .	25
<b>4</b>	<b>Conclusion</b>	<b>34</b>
4.1	Summary of the results . . . . .	34
4.2	Outlook on further experiments . . . . .	35
	<b>Bibliography</b>	<b>39</b>

# 1 Introduction

Tailoring an ultrafast light triggered optical switch that can be used many thousand of times while being stable under other external stimulations is the ultimate goal that application based research aims for when considering photochromisms in molecules. The word ultrafast typically implies dynamics on time scales in the picosecond to femtosecond time regime and photochromisms are defined as reversible transformations within a chemical compound upon irradiation with light<sup>1</sup>. Using ultrafast pump-probe spectroscopy it has been shown in the literature<sup>2</sup> that the cis-trans isomerization of azobenzene dissolved in ethanol takes place with a time constant of 170 fs and the trans-cis isomerization with a time constant of 320 fs. A throughout understanding of the isomerization process is desirable in order to exploit its dynamics for ultrafast photoswitching applications between the trans and cis state schematically displayed in figure 1.1. Since the switching of the conformation is accompanied by changes in many optical properties such as the refractive index, the dipole moment and the absorption spectrum<sup>1</sup>, azobenzene is a highly interesting object for scientific research. The possibilities to use the photochromism of azobenzene containing liquid crystals for image storage<sup>3</sup> and azobenzene derivatives for high density photoelectrochemical information storage<sup>4</sup> are just two examples of the versatility of this molecule.

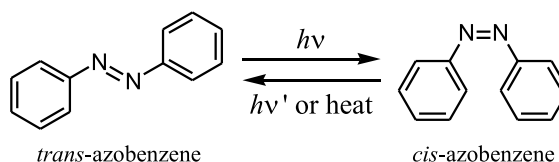


**Figure 1.1:** Chemical structure formula of the two isomers of the  $C_{12}H_{10}N_2$  molecule with the trivial name azobenzene. It consists of two phenyl rings that are attached to an  $N=N$  doublebond. The indicated isomerization process between the trans and cis state upon ultrafast excitation of azobenzene within polymer surroundings is the cornerstone of this thesis.

An important step to the aspired applications is an understanding of the reaction dynamics in various surroundings. Results of the ultrafast reaction dynamics of azobenzene in solution have been previously presented in the literature<sup>1,2,5</sup>.

For this thesis I applied spin assisted layer-by-layer deposition to a commercial polyelectrolyte called PAzo that contains azobenzene within the side groups attached to the polymer backbone. Thereby I created solid phase samples that incorporate azobenzene in thin films of polymers on top of quartz substrates. The goal of the experiments in this thesis is to compare the results of the steady state spectroscopy as well as the time resolved transmission spectroscopy of my azobenzene-polyelectrolyte thin film samples with results that have been reported for azobenzene in solution and comparable azobenzene-polymer-composites in the literature. Thereby I aim to study the effect of the polymer surrounding on the dynamics of the molecule. In addition I conducted experiments that enable us to investigate whether the PAzo layer undergoes an expansion or compression upon excitation with femtosecond laser pulses via stimulated Brillouin backscattering processes.

## 1.1 Structure of this thesis

- Chapter 1 provides a short summary of the used literature and the results reported for other systems containing azobenzene that inspired the conducted experiments. The presented papers are the general foundation upon which we build our theories for this thesis.
- In Chapter 2 I give a brief description of the preparation process of my samples and present measurements of their steady state transmission spectra, which indicate the possibility of reversible photoswitching.
- Chapter 3 contains the ultrafast processes of the thin film azobenzene samples, which are the main part of this thesis. In section 3.1 I introduce the general setup for pump-probe spectroscopy measurements. Experiments on the ultrafast changes in the transmission spectrum are presented in section 3.2 where I examine the decay of the transient absorption in the sample by probing within the first 20 ps after excitation. The second time resolved experiment presented in section 3.3 probes a strain pattern propagating into the substrate that is generated by the optomechanical response of the isomerization process. The interference condition and the theoretical background that enables us to detect this process is discussed in section 3.3.1. By comparing the phase of the interference pattern measured on the thin azobenzene-polyelectrolyte film with the phase of a sample with familiar expansion characteristics one can in principle classify the expansion behavior of azobenzene perpendicular to the substrate polyelectrolyte interface upon excitation with a femtosecond laser pulse.
- In Chapter 4 I summarize the results of the previously presented experiments leading to the tentative conclusions, which can be verified and elaborated by possible further experiments and applications that are presented as an outlook.

## 1.2 Motivating literature

The experiments I have conducted closely tie in with experience that has been previously gathered in the Ultrafast Dynamics in Condensed matter group at the University of Potsdam as well as published articles that are summarized in the following section.

### Characteristic absorption bands of the azobenzene unit

The incentive to closely study the behaviour of azobenzene has been given by the interesting dynamics of azobenzene presented by Nägle et al.<sup>2</sup> and Lednev et al.<sup>5</sup> who studied dissolved azobenzene with ultrafast pump-probe spectroscopy methods in ethanol and n-hexane, respectively. A review article of the field of ultrafast dynamics of photochromic systems has been published by Tamai et al.<sup>1</sup>. From there we know that azobenzene molecules show two absorption bands in the UV-Vis spectrum that can be attributed to the excitation of one of the lone pair electrons of the nitrogen atoms to an anti-bonding orbital ( $n\pi^*$ -transition) or the transition of one electron from the nitrogen  $\pi$  bond to an anti-bonding  $\pi^*$  orbital ( $\pi\pi^*$ -transition). The static absorption maxima in n-Hexane have been found at 445 nm and 315 nm for the  $n\pi^*$ -transition band and the  $\pi\pi^*$ -transition, respectively<sup>5</sup>. In ethanol one finds a broad  $n\pi^*$ -transition band with a maximum intensity at  $\lambda_{n\pi^*} = 435$  nm and two separated  $\pi\pi^*$ -transition in the UV at  $\lambda_{\pi\pi^*cis} = 275$  nm,  $\lambda_{\pi\pi^*trans} = 330$  nm. According to the results of ab initio calculations presented in figure 1.2 done for the azobenzene energy levels the energetic ground state is the trans configuration. Starting from molecules in the trans state it has been shown that the trans-cis isomerization can be triggered by static

irradiation of the molecules with light that has a wavelength within the  $n\pi^*$ -transition band of the valence electrons. From the excited  $S_1$  state the molecule can relax back to either the stable trans configuration or the metastable cis-configuration creating a dynamic equilibrium between both isomers.<sup>2,5</sup>

	$\lambda_{n\pi^*\text{trans}}$ $S_{0\text{trans}} \rightarrow S_1$	$\lambda_{n\pi^*\text{cis}}$ $S_{0\text{cis}} \rightarrow S_1$	$\lambda_{\pi\pi^*\text{trans}}$ $S_{0\text{trans}} \rightarrow S_2$	$\lambda_{\pi\pi^*\text{cis}}$ $S_{0\text{cis}} \rightarrow S_2$
n-hexane solution	445 nm		315 nm	
ethanol solution	435 nm		330 nm	275 nm
BMBA	440 nm	440 nm	320 – 350 nm	260 – 300 nm
$\epsilon$ [ $\text{M}^{-1} \text{cm}^{-1}$ ]	400	1500	20000 – 30000	7000

**Table 1.1:** Characteristic absorption bands for azobenzene in n-hexane<sup>5</sup>, in ethanol solution<sup>2</sup> and for 4-butyl-4'-methoxyazobenzene (BMBA)<sup>1</sup> as reported in the literature. The molar extinction coefficient  $\epsilon$  of the BMBA transitions is provided to representatively quantify the relative strength of the  $\pi\pi^*$ -transition<sup>1</sup>.

### Transient absorption characteristics of azobenzene in solution

With the characteristics of the steady state absorption spectra in mind one can move on to characterize the azobenzene thin polyelectrolyte film samples via pump-probe spectroscopy. Thereby the population of an excited state can be detected as a transient change in the absorption that decays over time after the excitation with the pump pulse. The transient absorptions of the electronic system in the  $S_1$  potential energy surface have been reported to decay with a time constant of 2.1 ps<sup>5</sup> in n-hexane and a double exponential decay with the time constants of 0.32 ps and 2.1 ps has been published for azobenzene in ethanol<sup>2</sup>. Upon excitation to the  $S_2$  potential energy surface a decay process with three different exponential components with the time constants  $\tau_1 \leq 0.2$  ps,  $\tau_2 = 0.9$  ps and  $\tau_3 = 15$  ps has been reported in the literature<sup>5</sup>. They are tentatively assigned to a relaxation of the first formed state  $S_2 \rightarrow S_2^\dagger$  ( $\tau_1$ ), the time it takes for an internal conversion process  $S_2^\dagger \rightarrow S_1^\dagger$  ( $\tau_2$ ) and the relaxation to the ground state  $S_1^\dagger \rightarrow S_0$  ( $\tau_3$ ). Excitation with an energy that places the system in an intermediate state between the  $S_1$  and  $S_2$  energy level has been found to add an additional decay channel with a time constant of 0.6 ps to the reported mono-exponential decay  $S_1 \rightarrow S_0$  in the transient absorption<sup>5</sup>. Figure 1.2 schematically summarizes the decay mechanisms and the time constants that have been reported for trans azobenzene in n-hexane solution, to which I aim to compare my measurements. For azobenzene in solution it is proposed in the literature that the excitation of the  $n\pi^*$ -transition leads to an isomerization via an inversion, whereas the isomerization via rotation is favored upon excitation of the  $\pi\pi^*$ -transition<sup>5,1</sup>. It has been noted that the steric effects can influence the isomerization pathways as it is the case in ringlike azobenzenophanes, where the rotation pathway is prohibited by steric hindrance<sup>1</sup>. In my thesis I recorded the static as well as the time resolved measurements on azobenzene incorporated into a polymer surrounding to see how the polyelectrolyte matrix influences the spectral position and the decay times of the azobenzene absorption bands.

### Spin assisted layer-by-layer deposition

For the sample preparation I used spin assisted layer-by-layer deposition that Kiel et al.<sup>7</sup> have proven to be a suitable method for preparing polyelectrolyte samples. Our group has already applied this method to integrate gold nanoparticles into a polymer matrix and achieved high structural perfection that has been verified by atomic force

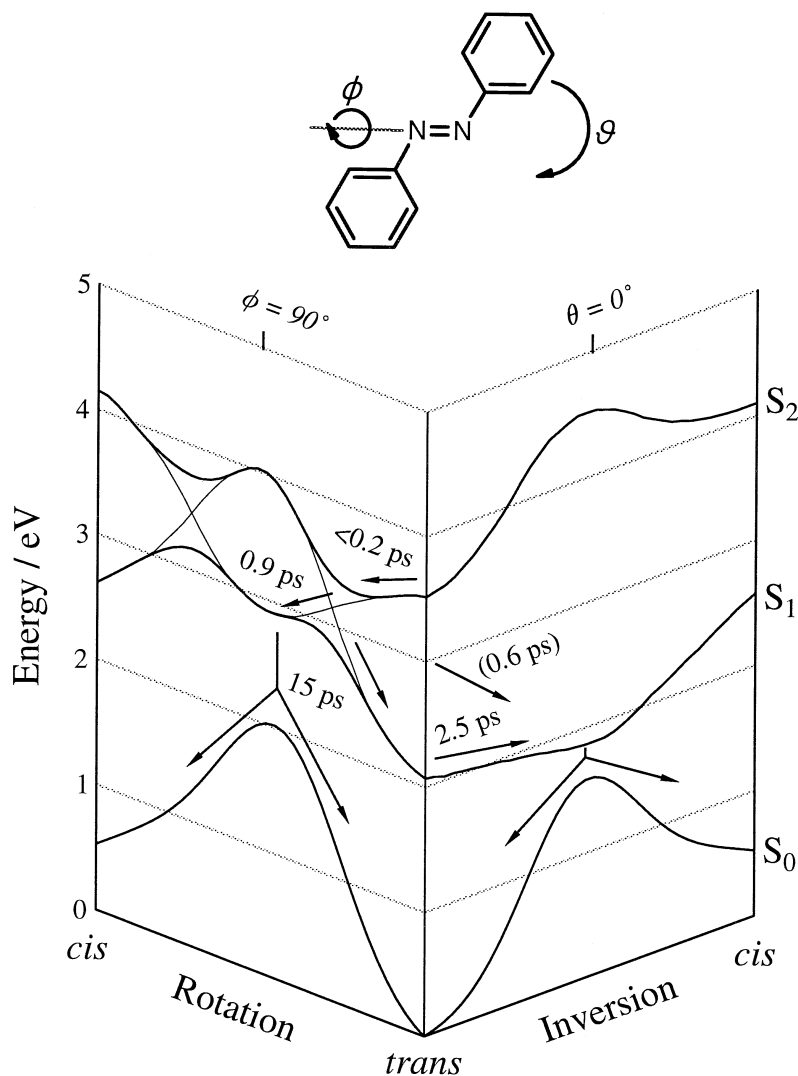


**Figure 1.2:** The top part of the graphic schematically shows the two possible isomerization pathways of azobenzene: the rotation around the double bond associated with the angle  $\phi$  and inversion at one of the nitrogen atoms associated with the angle  $\theta$ . Underneath one sees the potential energy surface of azobenzene in the *cis* as well as *trans* conformation that has been theoretically derived by Monti et al.<sup>6</sup> and adapted to the experimental results in n-Hexane solution<sup>5</sup>. The diagram shows the potential relaxation pathways as well as the associated time constants for each transition upon excitation from the *trans* ground state to the  $S_2$  potential energy surface. Excitation of the  $n\pi^*$  transition with a pump wavelength of 445 nm brings the electronic state to the  $S_1$  energy level, whereas the excitation of the  $\pi\pi^*$ -transition at 315 nm excites the electrons to the energy surface  $S_2$ <sup>5</sup>. A similar version has also been adapted for *cis*-azobenzene dissolved in ethanol<sup>2</sup>.

microscopy (AFM), X-ray reflectivity (XRR) and transmission electron microscopy (TEM) experiments<sup>7</sup>. For my experiments I applied the established routine but incorporated PAzo instead of the gold particles as the optically active constituent. The details of the preparation process and the used chemicals are briefly discussed in chapter 2.

### **Stimulated Brillouin oscillations**

In the second part of the presented time resolved experiments I detect the switching of the azobenzene molecules from trans to cis by the bipolar strain pulse that the thin layer sends into the substrate upon photo-excitation. Our approach to monitor the propagating strain pulse by ultrafast pump-probe spectroscopy is based on the experimental technique described by Thomson et al.<sup>8</sup>, which was recently further developed for multichannel measurements by Pontecorvo et al.<sup>9</sup>.

### **The pump-probe spectroscopy setup**

Last but not least Kiel et al. have measured the transient optical complex dielectric function of a gold-nanoparticle-polyelectrolyte composite with a setup similar to the one used in my experiments<sup>10</sup>.

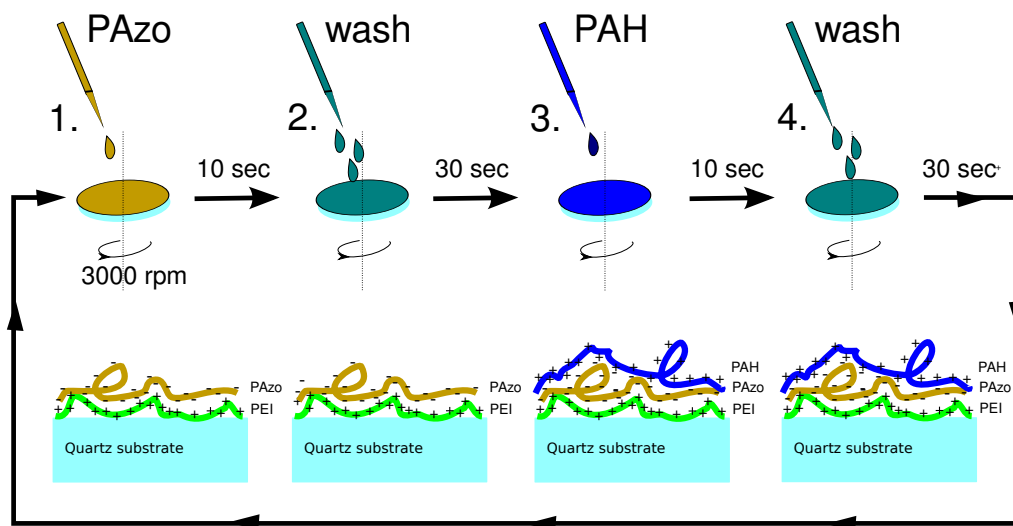
The presented knowledge and the listed publications form the basis of the conducted experiments in my thesis.

## 2 Preparation and sample characterization

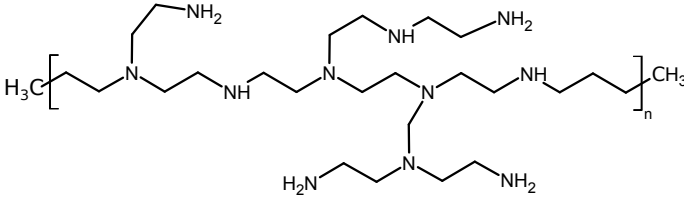
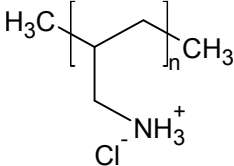
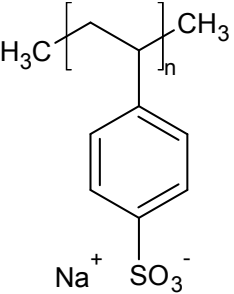
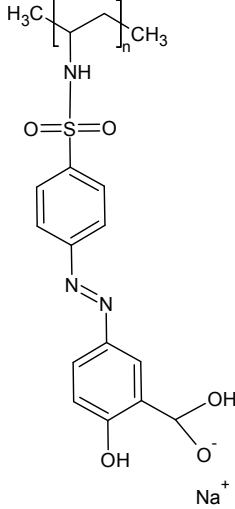
In my experiments I investigate layers of polyelectrolytes attached to a quartz substrate. A polyelectrolyte is a polymer where the repeating units carry an electrolyte group that dissociates in solution. The dissociated polyelectrolyte group leaves the polymer charged so that other charged polymers can be bound via electrostatic interactions. For polyelectrolytes spin-assisted layer-by-layer deposition has been proven to be a suitable method to create samples with high structural perfection<sup>7</sup>. After preparation I characterized the samples by transmission spectroscopy. Consequently I gained some insight about the characteristic absorption that is relevant to the ultrafast experiments presented in chapter 3.

### 2.1 Spin assisted layer-by-layer deposition

For the following experiments I prepared thin polyelectrolyte films on a quartz substrate that incorporate azobenzene into a structure of well defined polymer layers. All thin film polyelectrolyte samples used in this thesis are prepared by spin-assisted layer-by-layer assembly. An overview of the chemical characteristics of the used polyelectrolytes PEI, PAH, PSS and PAzo is given in table 2.1.



**Figure 2.1:** Schematic representation of the used preparation cycle for spin-assisted layer-by-layer deposition. A drop of dissolved polyelectrolytes having the opposite surface charge as the previous layer is brought on the sample where it spreads due to the rotation of the substrate at 3000 revolutions per minute (rpm). The polyelectrolytes attach by replacing the coulomb bonds of the dissolved  $\text{Na}^+$  or  $\text{Cl}^-$  counter ions of the present layer in an entropy driven process<sup>11</sup>. After each application the excess polyelectrolytes are washed off by deionized water and left to dry so that the next polyelectrolyte layer with opposite surface charge can be applied.

Abbreviation	PEI	PAH	PSS	PAzo
Chemical structure				
Chemical name	poly(ethyleneimine)	poly(allylamine hydrochloride)	poly(sodium 4-styrenesulfonate)	poly(1-(4-(3-carboxy-4-hydroxyphenyl)-azobenzene-sulfonamido)-1,2-ethanediyl)
Surface charge	positive	positive	negative	negative
Solvent	purified water (Milli-Q)	purified water (Milli-Q)	purified water (Milli-Q)	purified water (Milli-Q)
Concentration of polyelectrolyte	1,0 % wt	0,1 % wt	0,1 % wt	0,1 % wt
Additional NaCl	none	1M	1M	0.2M
Degree of polymerization	60000	58000	70000	unknown
Sum formula	$[C_{24}H_{59}N_{11}]_n$	$[C_3H_8NCl]_n$	$[C_8H_7SO_3Na]_n$	$[C_{17}H_{14}SO_5Na]_n$
Molecular weight of monomer unit $M_w$	501.6 $\frac{g}{mol}$	93.56 $\frac{g}{mol}$	206.2 $\frac{g}{mol}$	369,33 $\frac{g}{mol}$

**Table 2.1:** Summary of the chemical properties of the used polyelectrolytes

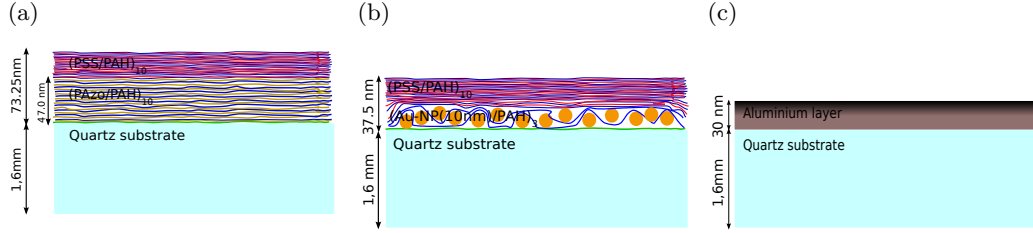
The preparation method I used closely follows a routine developed in the group of Bargheer<sup>7</sup>. After cleaning the surface of the quartz substrate with ethanol in an ultrasonic bath the substrate is mounted to a spin-coating machine and the layers of polyelectrolytes are successively applied. The first layer is always made of PEI that adsorbs to the quartz surface thanks to its branched structure, which creates a big surface for interactions with the substrate. In aqueous solution the amino groups in the polymer become protonated and thus form a polycationic molecule. To this positive surface charge alternating layers of anionic and cationic polyelectrolytes can be attached by electrostatic interactions in a cyclic routine. The replacement of the many dissolved  $\text{Na}^+$  or  $\text{Cl}^-$  counter ions of relatively low molecular weight by polyelectrolytes of opposite surface charge is an entropy driven process<sup>11</sup>. The entropy is increased by the replacement of the small  $\text{Na}^+$ ,  $\text{Cl}^-$  ions from their electrostatic bond partners at the polyelectrolyte layer, which adds more degrees of freedom to the system than the binding of the new polyelectrolyte layer consumes<sup>7</sup>. In addition a layered polyelectrolyte structure increases the hydrophobic effect of polymer backbones, which causes a dissociation of the water molecules and that adds even more degrees of freedom to the system<sup>11</sup>.

One cycle of the preparation routine for a double layer of polyelectrolytes is schematically depicted in figure 2.1. While spinning the sample at 3000 rpm a dissolved chemical with opposing surface charges compared to the current configuration is applied for 10 s in order to evenly adsorb to the surface. In between each application the surface is rinsed with purified water and spun for 30 s so that non-adsorbed molecules, which would hinder the sticking process of further layers, are removed. Due to their negative surface charges PSS and PAzo molecules will be attracted to the PEI and PAH polymers that have positive surface charges and vice versa. The process is repeated until the desired number and configuration of layers for the investigated samples is achieved. A modification of this method can also be used to incorporate gold nanoparticles, which are prepared to carry a negative surface charge, into a polymer matrix. The preparation and characterization of the gold nanoparticles within the polymer compound has been previously described in detail by Kiel et al.<sup>7,12</sup>.

As reference samples for the stimulated Brillouin backscattering experiments presented in section 3.3 I prepared a thin gold-nanoparticle-polyelectrolyte composite by spin assisted layer-by-layer deposition. In addition I used a thin aluminium film that is supposed to have a thickness of approximately 30 nm according to the calibration of the thermal evaporation unit. All samples are prepared on identical quartz substrates. The composition of the samples is summarized in table 2.2 and schematically depicted in the following figure 2.2.

The cylindrical quartz discs used as substrate have a diameter close to 2.5 cm and a thickness of approximately 1.6 mm. The thickness of each double layer of (PAH/PSS) polyelectrolytes has been determined to be 2.5 nm<sup>11</sup> and we assumed the thickness of a mono layer of PEI to be approximately 1.25 nm. Furthermore I measured the thickness of a double layer (PAH/PAzo) to be roughly 4.7 nm by applying atomic force microscopy to an intentionally scratched sample of 30 double layers (PAH/PAzo). According to the commercial supplier Sigma Aldrich the gold-nanoparticles have a diameter of approximately 10 nm. Thus they contribute roughly 10 nm to the total thickness of a thin polyelectrolyte film, since atomic force microscopy measurements have proven that they form monolayers under a comparable preparation routine<sup>7</sup>. Adding the thickness of each component of the used thin films leads to the estimation of the film thickness listed in table 2.2.

Name of sample	Important constituent	constitution of the sample	estimated film thickness
APazo2	PAzo	substrate/PEI(PAzo/PAH) <sub>10</sub> (PSS/PAH) <sub>10</sub>	73.25 nm
AAu	Au	substrate/PEI(Au-NP/PAH) <sub>3</sub> (PSS/PAH) <sub>10</sub>	40 nm
SAI	Al	substrate/Al	30 nm

**Table 2.2:** Overview of the composition of the used sample types**Figure 2.2:** Schematic of the used samples that all consist of a thin film attached to the same type of quartz substrate. (a) APazo2: a polyelectrolyte thin film containing 10 double layers of (PAzo/PAH) with a cap of 10 double layers of the transparent polyelectrolytes (PSS/PAH), (b)AAu: a gold-nanoparticle-polyelectrolyte composite, (c)AAl: an aluminium layer

## 2.2 Steady state transmission spectroscopy

Steady state transmission spectroscopy at a commercial UV-Vis transmission spectrometer (VARIAN CARY 5000) is carried out in order to characterize the used samples. The spectrometer provides us with the possibility to monitor the change in the transmission spectra before and after UV light irradiation. The results indicate a reversible photoswitching.

### 2.2.1 Transmission spectra of the used samples

In preparation of the time resolved experiments I measured the transmission spectra of the used samples. The results are shown in figure 2.3. From the transmission spectra we see that the quartz substrate is suitable for experiments in the visible and near ultraviolet spectrum since it is transparent in the wavelength range from 250 nm to 800 nm. Adding 10 double layers of (PSS/PAH) polyelectrolytes does not significantly change the transmission spectra in the relevant part of the UV-Vis spectrum. The gold-nanoparticle-polyelectrolyte sample exhibits a transmission in the range of approximately 65-80% with one pronounced minimum at a wavelength of 580 nm. This transmission decrease can be attributed to the plasmonic absorption of the gold-nanoparticles in the polyelectrolyte composite. The relatively broad plasmonic absorption indicates a clustering of the gold nanoparticles within the polyelectrolyte. The influence of the surroundings on the plasmonic peak have been studied in our group and a redshift of the resonance has been detected when the nanoparticles are covered with polyelectrolytes as it is the case in my samples<sup>12</sup>. The thin aluminium layer shows a relatively small transmission in the visible spectrum ranging from 5 to 15%.

In order to identify the measured transmission characteristics of the PAzo samples I compare the obtained transmission spectra of my azobenzene samples at first to studies on azobenzene in solution<sup>2,5</sup> where the absorption bands are well pronounced with reported absorbances  $A$  of up to  $A = 1.6$ . The absorbance of a liquid at a specific wavelength is defined in connection with the Lambert-Beer law for the transmittance  $T_\lambda$  stated in

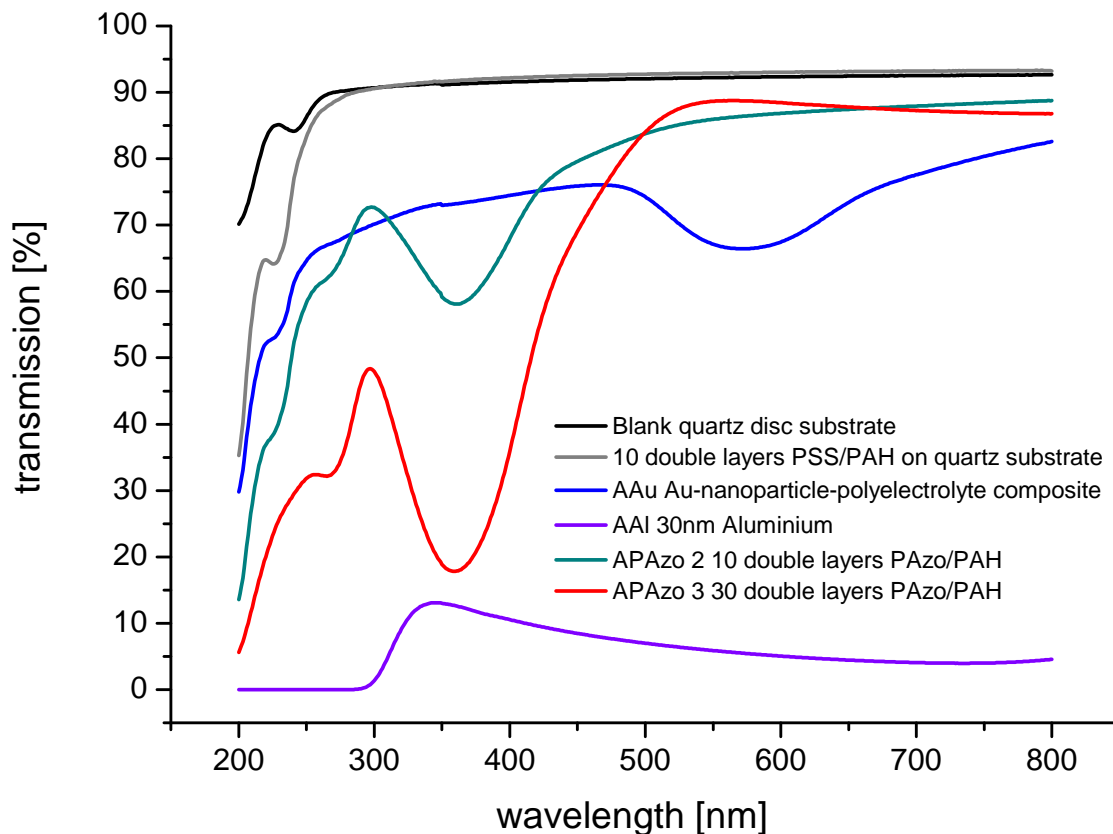


**Figure 2.3:** Transmission spectra of all samples used in my experiments. The quartz substrate is essentially transparent showing a transmission of 90% down to a wavelength of 250 nm, where it limits the transmission of all samples. 10 double layers of PSS/PAH polyelectrolyte exhibit no further decrease in transmission within the relevant UV-Vis spectrum. The AAu sample shows a characteristic transmission decrease at 580 nm that can be attributed to the plasmonic absorption of the gold nanoparticles. The aluminium layer is relatively nontransparent showing a transmission of less than 15%, which I attribute to its high reflection coefficient. The samples containing PAzo show one pronounced transmission minimum at 365 nm that is linked to the  $\pi\pi^*$ -transition of the trans configuration of the azobenzene molecules.

equation 2.1.

$$T_{\lambda} = \frac{I}{I_0} = 10^{-A_{\lambda}} = 10^{-\epsilon \ell c} \quad (2.1)$$

In this context  $\epsilon$  is the extinction coefficient,  $\ell$  is the optical pathlength through the absorbing medium and  $c$  stands for the concentration of the solution.

My samples containing PAzo show one pronounced transmission minimum at 365 nm. From the potential energy plot presented in figure 1.2 we expect two different possible transitions that require energies in the examined UV-Vis spectral range. The  $n\pi^*$ -transition is located in the visible spectrum and the  $\pi\pi^*$ -transition in the ultraviolet range. Both transitions can possibly have a trans- and cis contribution. The steady state absorption of trans azobenzene has been reported to have the  $\pi\pi^*$ -transition band at approximately 315 nm that has a 40 times larger absorbance as the  $n\pi^*$ -transition found at approximately 450 nm in hexane solution<sup>5</sup>.

In ethanol solution two energetically separated components of the  $\pi\pi^*$ -transition have been reported<sup>2</sup> at  $\lambda_{\pi\pi^*trans} = 330$  nm and  $\lambda_{\pi\pi^*cis} = 275$  nm. In addition the reported  $n\pi^*$ -transition between 380 nm and 520 nm has a contribution from the trans as well as the cis state but the extinction coefficient for the  $n\pi^*$ -transition  $\epsilon_{cis} = 1470 \text{ M}^{-1}\text{cm}^{-1}$  is approximately 3.5 times larger for the cis configuration as for the trans configuration  $\epsilon_{cis} = 405 \text{ M}^{-1}\text{cm}^{-1}$  in ethanol solution. Based on these findings I assign the transmission minimum that I measured at 365 nm to the  $\pi\pi^*_{trans}$ -absorption because it is the dominant feature in all reported spectra. The wavelength shift of the  $\pi\pi^*_{trans}$ -band between the reported results in solutions and my measurements is consistent with a solvatochromism that shifts the absorption to lower energies with increasing polarity of the surrounding. That the polarity of the solvent effects energy levels of the dissolved molecules and thereby shifts the absorption bands is well established although its quantitative prediction is complicated<sup>13</sup>. Hexane has the lowest polarity of the used surroundings (dielectric constant  $\epsilon = 1.9$ ) due to its unpolar alkane structure, whereas ethanol molecules possess a polar OH group that leads to a larger polarity ( $\epsilon = 24$ ) of the molecule<sup>14</sup>. We expect the polyelectrolyte matrix of my thin film samples to be highly polar since the different layers are attached to each other via charged electrolyte groups. The order in the polarity of the different surroundings is consistent with the observed order in the  $\pi\pi^*_{trans}$ -absorption wavelengths:  $\lambda_{\pi\pi^*trans}(\text{hexane}) = 315 \text{ nm} < \lambda_{\pi\pi^*trans}(\text{ethanol}) = 330 \text{ nm} < \lambda_{\pi\pi^*trans}(\text{polyelectrolyte}) = 365 \text{ nm}$ . The solvatochromic red shift with increasing polarity of the surrounding medium is also confirmed by the literature<sup>14</sup>.

The transmission spectra for two types of thin film samples that have a very similar structure to the samples used in my experiments have also been reported in the literature by Toutianoush et al.<sup>15,16</sup>. Their samples have been prepared by layer-by-layer assembly via dip coating, which also yields alternating layers of polyelectrolytes containing azobenzene. In the first type of the polyelectrolyte samples azobenzene has been incorporated into the main chain of the polymer backbone<sup>16</sup>. In the second type of samples azobenzene has been integrated into dianions as well as dications linking cationic, respectively the anionic polyelectrolytes<sup>15,17</sup>. For those sample types the  $\pi\pi^*$ -transition has been reported to have its maximum at 360 nm and 350 nm respectively and the  $n\pi^*$ -transition appears as a small shoulder at 450 nm. These results are in good agreement with the spectral position of the  $\pi\pi^*$ -transition measured on my samples.

### 2.2.2 Reversible photoswitching in azobenzene thin films

Experiments by Toutianoush et al. on polyelectrolyte thin film samples containing azobenzene have shown that a reversible photo switching of the incorporated azobenzene molecules is possible via alternating irradiation with UV light ( $\lambda_1 < 370$  nm) that induces the trans-cis isomerization and that can be reversed via irradiation with light in the visible spectrum ( $\lambda_2 > 450$  nm)<sup>16,15,17</sup>. In solution as well as for the self assembled polymer structures the formation of the cis isomer is indicated by the reduction of the  $\pi\pi^*_{trans}$ -band in the ultraviolet spectrum and the appearance of the  $n\pi^*$ -band in the visible spectrum that has a dominant contribution from the cis configuration<sup>5,2,16</sup>.

Given this incentive I also briefly studied the changes in the azobenzene thin film transmission spectra that can be induced by irradiation with a UV-lamp with a wavelength of  $\lambda = 365$  nm and an energy flux of  $4 \text{ Wm}^{-2}$ . The absolute and relative changes in the transmission spectra induced by increasing irradiation on a PAzo2 sample are presented in figure 2.4.

The presented results in figure 2.4(a) show an increase in transmission at 365 nm upon irradiation, which is consistent with the predicted decrease of the  $\pi\pi^*$ -absorption. The appearance of the  $n\pi^*$ -band in the visible spectrum could not be identified, probably because the absorbance of this transition is small compared to the  $\pi\pi^*$ -transition. Nevertheless I observed a relaxation back to the trans conformation after irradiation of the sample with sunlight or resting it for three days. That indicates that the previously reported reversible photo switching is also possible within the prepared polyelectrolyte thin-film samples. Further experiments that aim to detect the cis conformation absorption band within the transmission spectrum as well as a polarization dependence in the transmission due to possible alignment effects of the molecular dipole moments are currently being conducted with a mercury vapor lamp that has a higher energy flux.

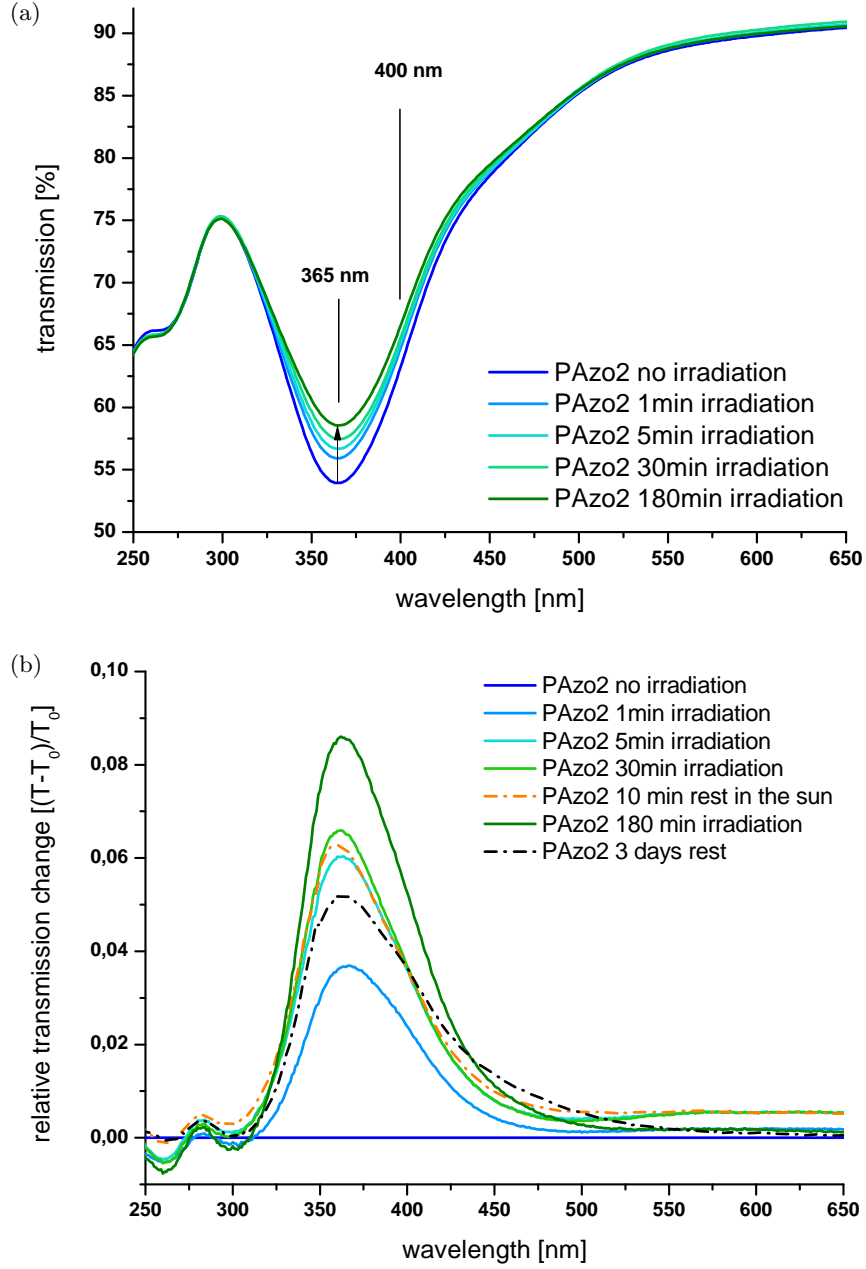


**Figure 2.4:** (a) Transmission spectra of the Pazo2 sample that contains 10 double layers of (PAzo/PAH) for different, consecutively increasing exposition times to UV irradiation at  $\lambda = 365$  nm (process from blue to green curves). The transmission consistently rises with the exposure time of the sample to the UV-irradiation as indicated by the arrow. Thin lines indicate the central wavelength of the  $\pi\pi^*$ -transition at 365 nm and the pump wavelength of 400 nm used in time resolved experiments in section 3. (b) Relative change in the transmission of the data presented in (a). One can see that the relative change has its maximum at the absorption band. Note that irradiation in the visible spectrum as well as resting the sample induces a decrease in the relative transmission change, which I associated with a relaxation of the azobenzene molecules from cis to trans.

## 3 Pump-probe spectroscopy

The main part of my experiments treats the ultrafast processes of azobenzene in polyelectrolyte thin films that are studied with optical femtosecond pump-probe spectroscopy presented in this chapter.

### 3.1 Experimental setup

For pump-probe spectroscopy short light pulses from two different beam paths have to overlap on the sample under investigation. The so called "pump pulses" are designed to induce a change in the sample, whereas the probe pulses are designed to optically measure the reflectance and transmittance of the sample on ultrafast time scales without introducing new dynamics. A schematic sketch of the pump-probe setup I used during the experiments is provided in figure 3.1.

The used laser pulses are generated by a 5 kHz regeneratively amplified titanium:sapphire-laser system from Spectra-Physics. It provides 140 fs laser pulses at a central wavelength of 795 nm with a power of 1.6 mW. A fraction of 440 mW is used to perform the pump-probe measurements. At the first beamsplitter 16 mW of the laser beam are separated from the pump beam for white light generation. The remainder afterwards passes the delay line whose length can be adjusted by an electronically operated stage. After the delay line the pump beampath crosses the chopper which blocks 50% of the pulses. The chopper consists of a disc with equally spaced windows that rotates within the beam and thus gates the pump pulses with a frequency of 250 Hz upon a trigger signal from the laser. The chopper is only introduced to the beam path of the pump beam and thus enables the user to alternately measure pumped and unpumped states of the sample. In the following the pump beam passes a beta-BaB<sub>2</sub>O<sub>4</sub> (BBO) non-linear optical crystal that is aligned for second harmonic generation. Thus approximately 50 mW of the incident beam are converted to light pulses with a wavelength of approximately  $\lambda = 400$  nm. The 400 nm light pulses created by the second harmonic generation process have a polarization perpendicular to the incoming light so that they are s-polarized with respect to the used plane of reflection. For some reflectivity measurements a  $\frac{\lambda}{2}$ -plate optimized for 400 nm was introduced into the beam in order to retain p-polarized pump light. The remaining light of the fundamental wavelength is discarded at a dielectric mirror whose reflection is optimized for the second harmonic by simultaneously having a high transmission at the fundamental. Finally the pump pulses are focussed on the sample by an achromatic lens with a focal length of  $f = 150$  mm to a spot size of approximately  $152 \mu\text{m} \times 195 \mu\text{m}$ . The maximum pump fluence was  $35 \frac{\text{mJ}}{\text{cm}^2}$ .

After separation from the pump beam the probe beam passes a  $\frac{\lambda}{2}$  plate which rotates the linear polarization of the laser pulses by  $90^\circ$  from p- to s-polarization in respect to the used plane of reflections. Afterwards the pump beam is used for femtosecond white light generation. For that it is focussed with a  $f = 30$  mm lens close to the damage threshold into a sapphire disc thereby creating high intensities within the material. Consequently highly nonlinear effects especially self-phase modulation take place and thus the pulse spectrum will be broadened considerably after passing the crystal<sup>18</sup>. The resulting spectrum is broad

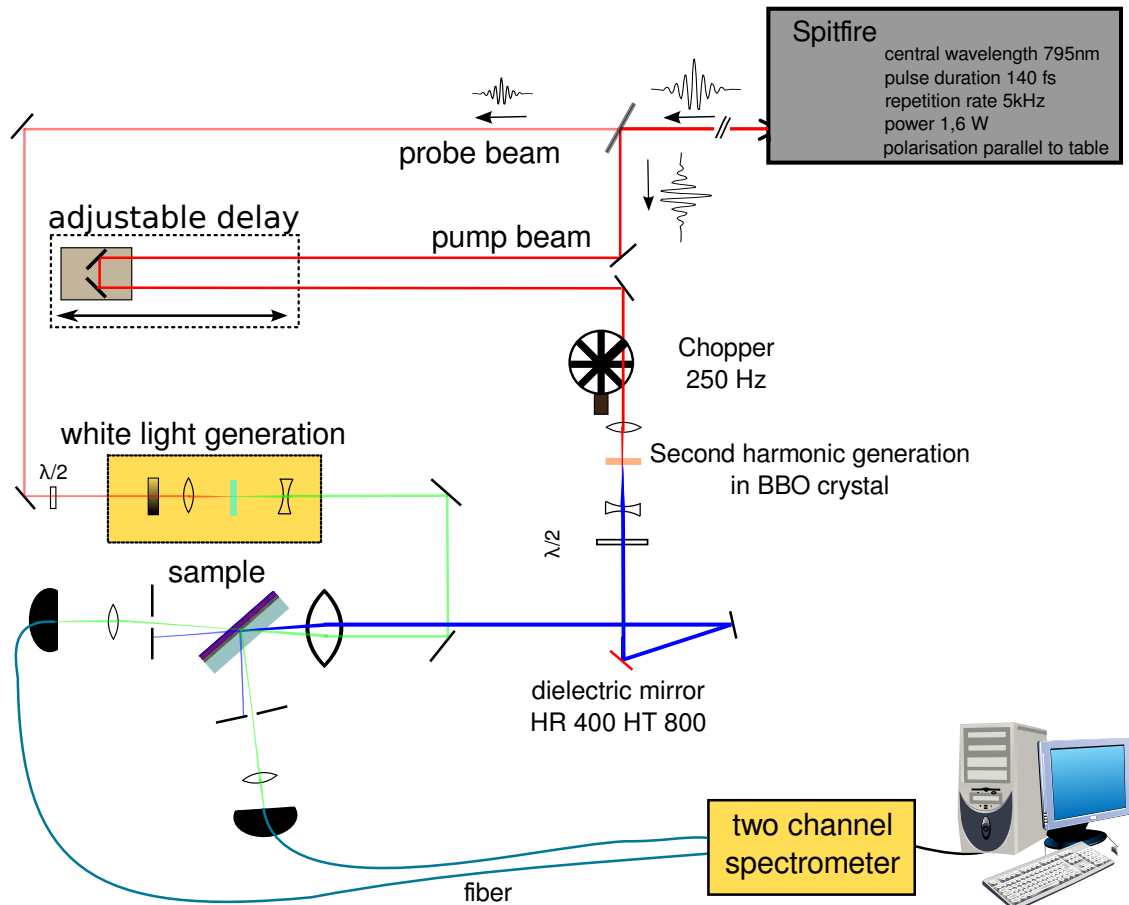


**Figure 3.1:** Schematic of the experimental setup used for pump-probe measurements. Femtosecond laser pulses are emitted at a central wavelength of approximately 795 nm and then split up into a pump and probe beam. The relative delay between the pulses can be adjusted via a variable delay line introduced into the pump beam path. The pump beam undergoes a second harmonic generation process in a nonlinear BBO crystal whereas the probe beam is submitted to white light generation. Both beams are brought to spatially overlap on the sample. The transmission and the reflection of the probe beam are coupled into different fibers leading to a two channel spectrometer that is operated via a LabVIEW programme. A chopper blocks fifty percent of the pump pulses enabling the user to measure the sample in the pumped and unpumped state within one cycle.

enough, typically ranging from 450 – 800 nm, so that the light appears white to the eye justifying the term "white light". The white light is focussed on the sample to spatially overlap with the pump beam. Due to the different angles of the incoming beam paths relative to the normal the reflections of the pump and probe beam can be well separated so that only the reflection of the white light is focussed into a fiber leading to a spectrometer. The spectrometer apparatus allows wavelength resolved measurements of the incoming light in the spectral region from 200 nm – 1000 nm with a resolution of 0.7 nm. Hence the created white light enables us to probe the reflection intensity of the sample in a broad region of the visible spectrum in a time efficient way within one measurement. For measuring the transient absorption I placed a spectrometer in transmission of the sample and determined the change in relative transmittance  $\frac{\Delta T}{T_0}$  defined as in equation (3.1):

$$\frac{\Delta T}{T_0} = \frac{T - T_0}{T_0} \quad (3.1)$$

where T stands for the measured transmission intensity of the pumped sample and  $T_0$  for the transmission intensity of the unpumped sample. A corresponding definition applies to the relative reflectivity change  $\frac{\Delta R}{R_0}$ . Using this setup it has been shown in our group that a simultaneous measurement of  $\frac{\Delta T}{T_0}$  as well as  $\frac{\Delta R}{R_0}$  enables the direct measurement of the dielectric function  $\epsilon(\omega, t)$  of a transparent sample, when the static component  $\epsilon(\omega)$  of the sample is known<sup>10</sup>.

The delay time between the pump and probe pulse on the sample can be adjusted by moving the translation stage. The delay time  $\Delta t$  is consequently defined as:

$$\Delta t = t_{\text{probe}} - t_{\text{pump}} \quad (3.2)$$

## 3.2 Relative transmittance measurements

### 3.2.1 Measurement and data analysis

Using the setup described in section 3.1 in the mode for measuring the change in the relative transmittance  $\frac{\Delta T}{T_0}$  on the APazo2 sample that contains 10 double layers of (PAzo/PAH) I obtained the data displayed in 3.2(a). In that graphic one can see that the instant of biggest relative transmittance change shifts in time within the measured spectrum. Since these changes are due to nonlinear interactions between pump and probe beam and consequently proportional to the intensity within the spatial overlap we define the moment of strongest change as best temporal overlap. Due to dispersion within beam guiding elements of the white light this moment is wavelength dependent. Consequently the instant of temporal overlap  $t_0 = 0$  ps has been determined for each wavelength by the maximum value of the absolute transmittance change signal in the sample. By subtracting the fitted time shift from the signal for each wavelength the moments of best temporal overlap coincide as displayed in figure 3.2(b).

Graphic 3.2(b) shows the dispersion corrected change in relative reflectivity of the APazo2 sample that contains 10 double layers of (PAzo/PAH). One can see large transmission changes at zero delay due to the nonlinear interactions mentioned earlier. After the nonlinear effects have passed at a delay of  $\Delta t = 300$  fs we detect a negative relative transmission change in the majority of the probe light spectrum. One can also see that the negative change decays over time. The relative transmittance change corresponds to a transient absorption of the investigated molecules. Representative cross-sections at different probe wavelengths are presented below in figure 3.2(c). The cross sections illustrate the strong intensity modulation around time zero that I interpret as nonlinear artefacts due to the

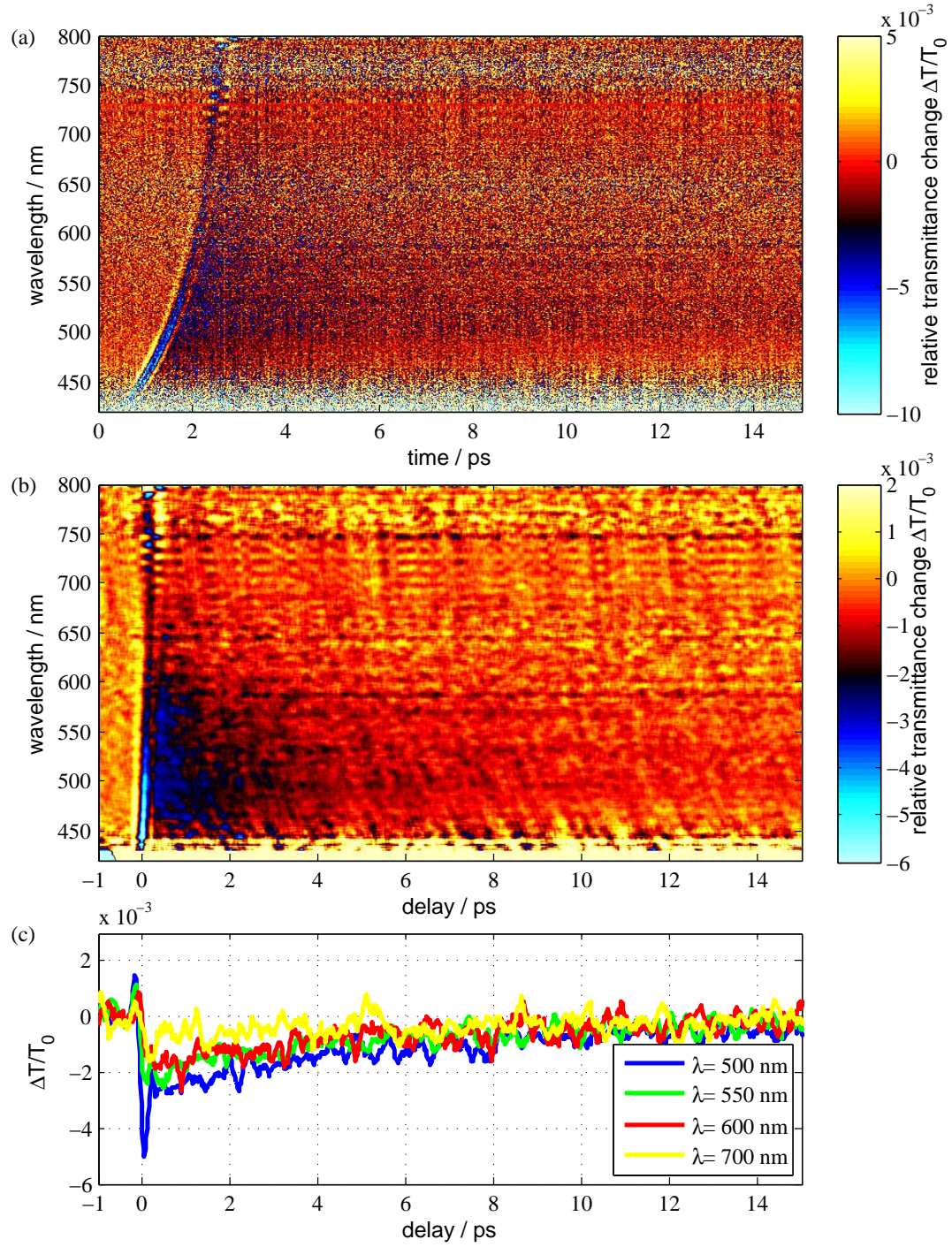


**Figure 3.2:** Relative transmittance change measured on the APazo2 sample that contains 10 double layers (PAzo/PAH): The uncorrected signal at delay times smaller than 15 ps (a) shows a pronounced rise of the intensity modulation of the relative transmittance change that is shifted in time with increasing wavelength.

The dispersion corrected transmittance change that was in addition smoothed over 5 nm in the wavelength domain and 200 fs in time is displayed in (b). All further evaluations and profiles are derived from these data. They show a strong relative change at zero delay between pump and probe over the measured range. Cross-sections of the data in (b) at different wavelengths are shown at the bottom (c) to provide a general idea of the shape of the signal.

high intensity within the spatial overlap. I also detected the signature of the nonlinear artefacts in measurements of a plain quartz substrate and from that I know that it is decayed after a delay time  $\Delta t = 300$  ps. Consequently I restrict my interpretation of the measurement to delay times greater than that.

### 3.2.2 Discussion of the results

For a first qualitative analysis of the transient absorption within the probe spectrum figure 3.3 shows the relative transmittance change at different time slices. There one can see that the relative transmittance change is predominantly present in the spectral range from  $\lambda = 450$  nm to  $\lambda = 650$  nm. The presented data is also consistent with the decay of the signal over time although a negative offset is still present after  $t = 15$  ps.

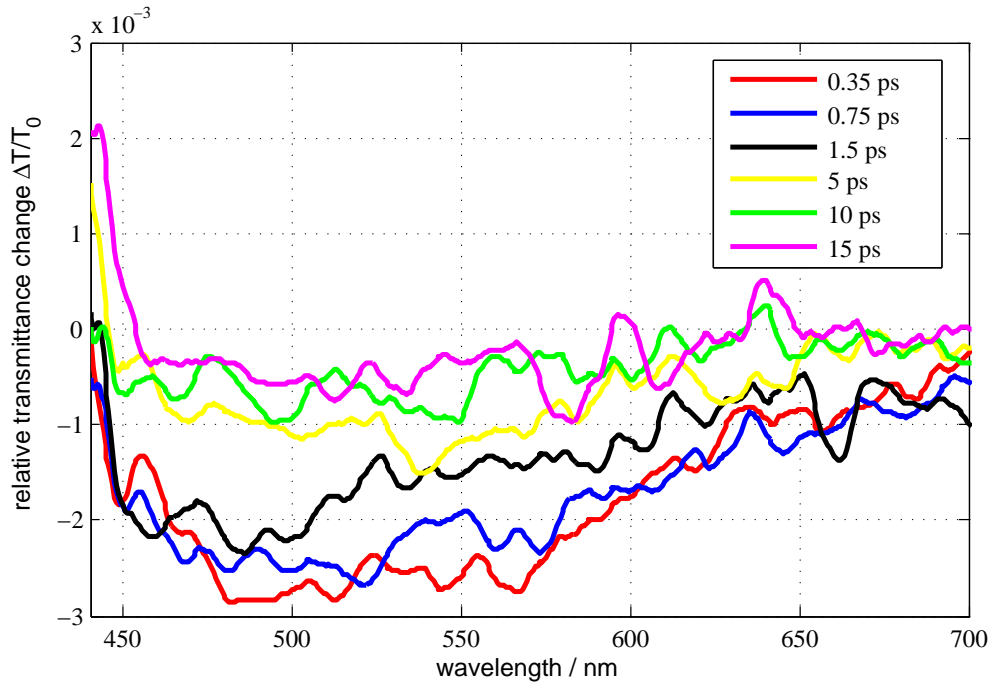


**Figure 3.3:** Relative transmittance change of 10 double layers (PAzo/PAH) plotted for different delay times showing a gradual decrease in the spectral region of 450 – 600 nm where the relative change is most pronounced. The presented data have been smoothed over a 10 nm interval in the wavelength domain for improved legibility.

Now I focus on the decay of the transient absorption at specific wavelengths and compare it to the data measured on azobenzene in n-hexane solution<sup>5</sup>. Due to the presence of the non-linear artefacts I do not expect to resolve fast decay constants smaller than 300 fs and therefore fitted slices at fixed wavelengths with a mono-exponential decay plus a constant offset for long lasting changes. The results of this procedure are displayed in figure 3.4.

Upon close examination of the data presented in figure 3.4 one can see that the mono-exponential fit shows a qualitative agreement. The determined time constants  $\tau_{470\text{ nm}} = 5.3$  ps,  $\tau_{500\text{ nm}} = 5$  ps and  $\tau_{575\text{ nm}} = 4$  ps for the exponential decay at three different wavelengths give a first quantitative impression of the relevant time scale for the transient absorption in the azobenzene thin polyelectrolyte films. From the overview plot of the relative transmission change displayed in figure 3.2(b) one can see that the sample exhibits

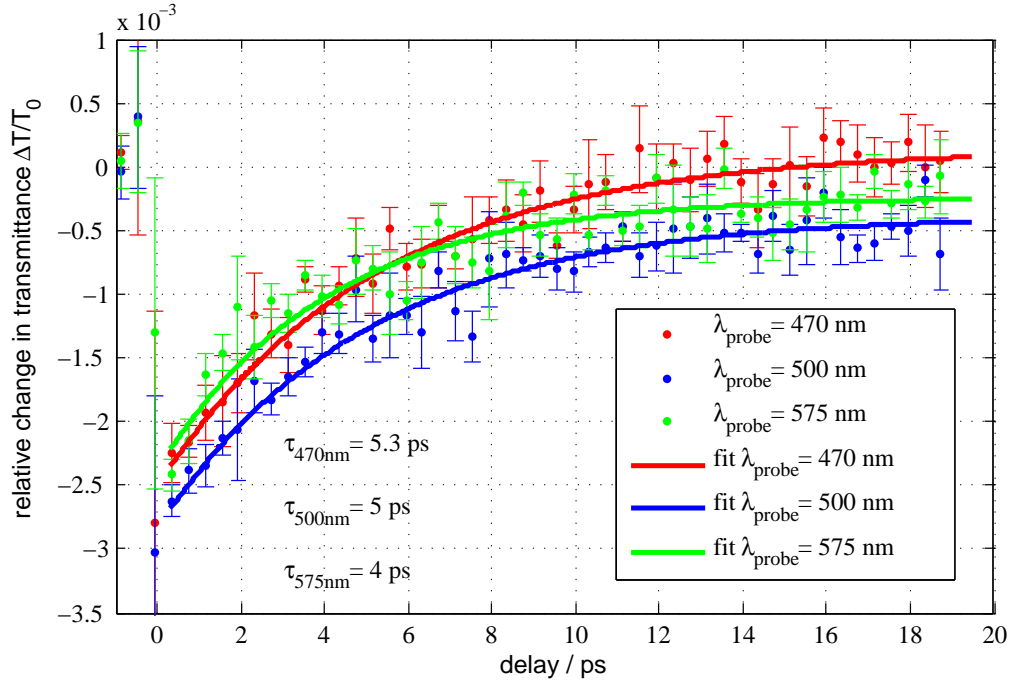


**Figure 3.4:** Decay of the relative transmittance change  $\frac{\Delta T}{T_0}$  measured on the APazo2 sample. The dots correspond to the measured relative change of 10 double layers (PAzo/PAH) plotted for three different probe wavelengths and smoothed over 0.200 fs in the time and 5 nm in the wavelength domain. After an abrupt change in the measured signal at zero delay the initial change decays over time. The errorbar contains one standard deviation of the grouping of points that correspond to the plotted data point. The solid lines represent mono exponential fits with a constant offset that qualitatively fit to the data after a delay of 400 fs. Note the offset present for delay times greater than 15 ps.

a response in the wavelength region from 450 – 650 nm. For each wavelength I fitted a mono-exponential decay of the type  $\frac{\Delta T}{T_0}(\Delta t) = Ae^{-\frac{\Delta t}{\tau}} + B$  to the signal starting at  $\Delta t \geq 400$  fs using the fit parameters Amplitude  $A$ , decay constant  $\tau$  and offset  $B$ . Figure 3.5 displays the fitted parameters in the relevant part of the probe spectrum. The fitted decay constants displayed in figure 3.5(a) are determined to be approximately  $5 \pm 1$  ps for the transient absorption process. As indicated by the thin line in figure 2.3(a) the used pump wavelength of 400 nm is located in long wavelength region of the  $\pi\pi^*$ -absorption band. Consequently I expect the electronic system of the azobenzene units in the polyelectrolyte matrix to be excited to the  $S_2$  potential energy surface with little excess energy left. For trans-azobenzene in n-hexane solution the relaxation process from this energy level has been reported in the literature to decay with three different time constants  $\tau_1 \leq 0.2$  ps,  $\tau_2 \approx 0.9$  ps and  $\tau_3 \approx 15$  ps<sup>5</sup>. There are obvious deviations in the time scale relevant for azobenzene in polyelectrolyte surroundings as compared to azobenzene in solution. None of the three reported time constants seem to even qualitatively agree with the time scale we determined for the thin polyelectrolyte sample. Although we have not expected to reproduce the same results from azobenzene in solution with azobenzene incorporated into a polymer matrix the differences are remarkable.

In addition we noticed a negative offset in the relative transmittance change that is persistent at delay times greater than 15 ps. Figure 3.5(b) shows the fitted offset  $B$  for the relevant probe wavelengths. There we see that the offset is most pronounced at probe wavelengths around 525 nm. At that particular wavelength the offset in the relative transmittance change is about  $5 \cdot 10^{-4}$ , which is roughly 25% of the amplitude  $A$  of the mono-exponential decay. The amplitude  $A$  of the transient absorption varies in between 0.35% and 0.15% over the relevant wavelength region as it is displayed in figure 3.5(c). The offset indicates another decay channel with an even larger decay constant that is present for azobenzene in the polyelectrolyte medium. For a first estimation of the additional time scale we recorded an additional scan with bigger time steps up to a delay time of 200 ps. The results are displayed in figure 3.6. The graphic shows that the relevant time scale at which all transient absorption changes decay to zero is approximately 60 ps.

Altogether we have now recorded the two relevant time scales  $\tau_1 \approx 5$  ps and  $\tau_2 \approx 60$  ps for the decay of the transient absorption of the azobenzene molecules in polyelectrolyte thin films. A tentative interpretation of the transient absorption measurements is that the binding of the azobenzene compound within the polymer strongly changes the potential energy landscape from the shape that I schematically displayed in the introduction in figure 1.2. It is furthermore possible that the complete isomerization via rotation is hindered by the surroundings. Possibly the azobenzene compounds start to isomerize due to the excitation but are forced back into the trans conformation by their binding partners. The influence of the attached binding partners is not present for pure azobenzene in solution for which the decay constants are published in the literature. Further investigation is needed in order to formulate precise statements concerning the decay mechanism as well as the additional larger time scale. Especially determining the decay times at the resonant pump wavelength for the  $\pi\pi^*$ -transition at approximately 365 nm and at 450 nm that is expected to excite the  $n\pi^*$ -transition should exhibit different characteristics that can be clearly assigned.

From my point of view a slower decay of the transient absorption as compared to results reported for experiments in solution is plausible due to the restrictive influence of the densely packed polymers that might partially inhibit the cis-trans isomerization of the molecules. A communication about so far unpublished experimental results with the

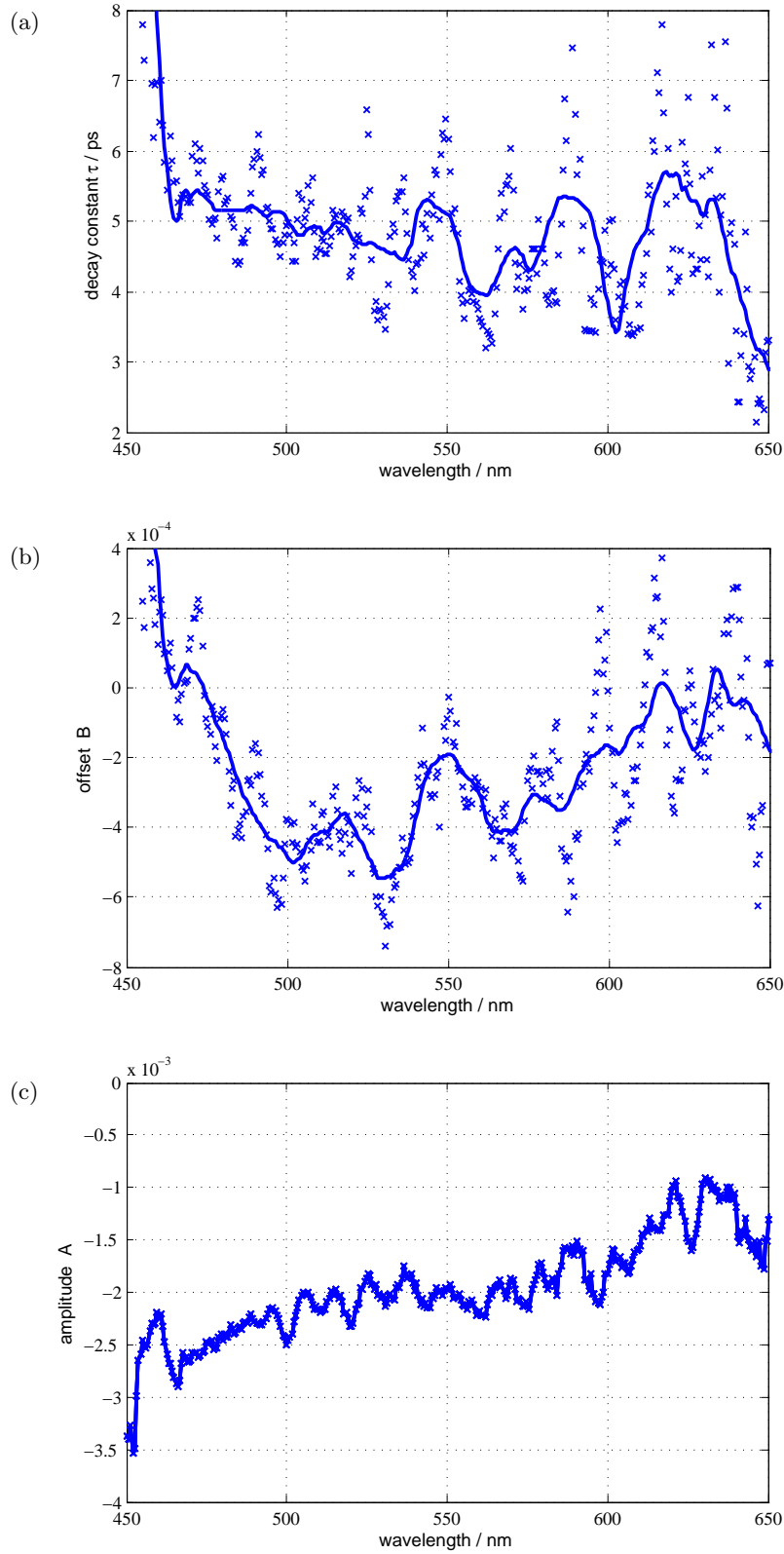


**Figure 3.5:** Crosses represent the fitted decay constants  $\tau$  (a), offset  $B$  (b) and amplitude  $A$  (c) of the transient absorption of a sample containing 10 double layers (PAzo/PAH) from a mono-exponential fit of the type  $\frac{\Delta T}{T_0}(\Delta t) = Ae^{-\frac{\Delta t}{\tau}} + B$  plotted against the probe wavelength. In (a) and (b) a running average over 25 nm has been added as guide to the eye. The majority of the decay constants in (a) has a value of approximately  $5 \pm 1$  ps. The fitted offset  $B$  is largest around 525 nm (b).

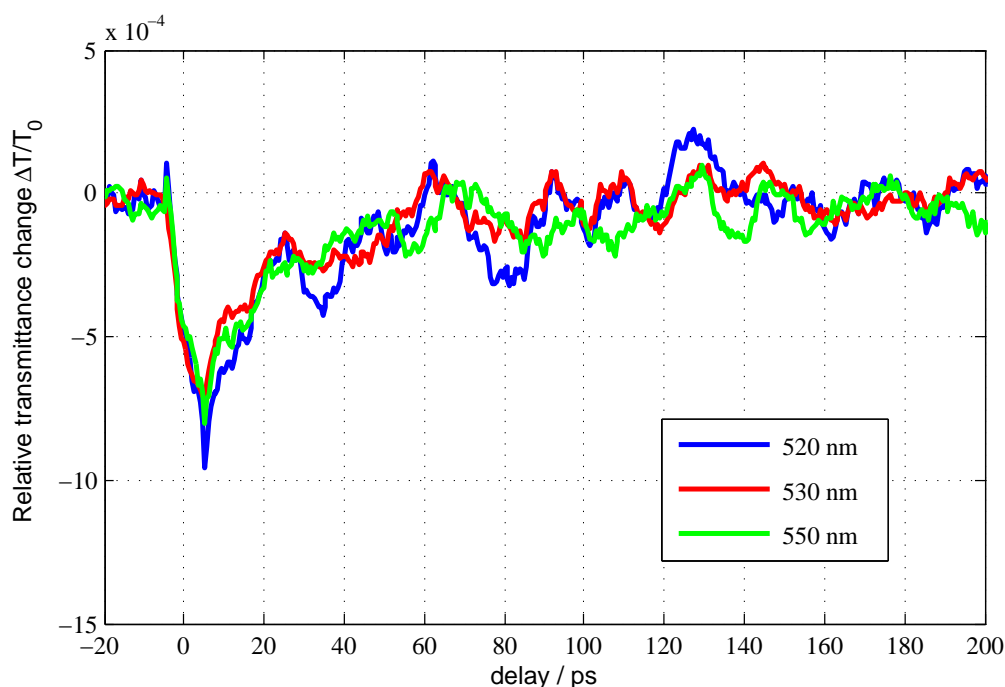


**Figure 3.6:** Measurement of the decaying transient absorption in a sample containing 10 double layers (PAzo/PAH). The data have been smoothed over 10 ps and 15 nm in the wavelength domain. One can see that the initial signal has decayed to approximately zero for the first time at a delay time around 60 ps

molecular physical chemistry group at the Christian-Albrechts-University in Kiel supports that hypothesis. They determined a similar time scale of 5.5 ps for the fluorescence lifetime of azobenzene that is incorporated into polymer colloids<sup>19</sup>. The identical azobenzene component without the colloid exhibited a fluorescence lifetime of only 0.5 ps<sup>19</sup>. That again underlines that the influence of possible attached substituents can not be neglected when comparing the decay constants of different azobenzene compounds.

### 3.3 Transient reflectivity measurements

Although the transient absorption dynamics of the azobenzene-polyelectrolyte thin films could also be studied in relative reflection measurements we now take a different approach by investigating the strain pulse that the excitation of the azobenzene molecule launches into the substrate. For that we exploit the induced relative reflectivity changes and compare our results to the excitation a thin aluminium films and a gold-nanoparticle-polyelectrolyte composite that are known to expand.

#### 3.3.1 Theoretical background to the Brillouin oscillation measurements

In the second part of the ultrafast pump-probe spectroscopy experiments I measure relative reflectivity changes with the setup described by Pontecorvo et al.<sup>9</sup> that corresponds to the reflection geometry of the setting described in section 3.1. For all relative reflectivity change measurements the samples were pumped and probed from the backside since I intend to study an effect in the substrate. The beam geometry for the different samples is

depicted in figure 3.7. The incident laser light enters the quartz substrate first at an angle of  $\alpha = 60^\circ$  relative to the surface normal, is diffracted according to Snell's law and is then partially reflected from the substrate thin film interface at the angle  $\beta$ . The reflected part leaves the substrate again at an angle of  $\alpha = 60^\circ$ . The static reflection from the quartz surface is spatially separated from the reflection on the interface and can be blocked at a distance of approximately 15 cm so that only the reflection from the thin layer is focussed into the fiber of the spectrometer. This reflection can then interfere with a third reflection from a strain pattern propagating into the substrate creating an oscillation in the relative reflectivity change that we intend to study further. The change in the refractive index in the substrate, which is necessary for a reflection is induced by a bipolar strain pulse originating from the expansion or compression of the top layer<sup>8</sup>. In metal transducers the strain is usually generated by the thermal expansion of the thin layer on top of the sample that has been excited by the pump laser beam<sup>9</sup>. After its creation the strain pulse propagates into the substrate at the speed of sound  $v_s$  of the substrate as a travelling plane from which the probe beam is partially reflected. The interference with the static reflection is not constant but oscillates with a period  $T$  and a corresponding Brillouin oscillation frequency  $\nu$  that can be derived by a Bragg condition according to figure 3.7.

Starting from the condition of constructive interference I can derive the oscillation frequency for the relative reflectivity change for each wavelength:

$$\lambda_{pr} = \frac{2v_s T n}{\cos(\beta)} \quad (3.3)$$

$$\Leftrightarrow \nu = \frac{1}{T} = \frac{2v_s n}{\lambda_{pr} \cos(\beta)} \quad (3.4)$$

where  $n$  is the real part of the refractive index of the substrate,  $\beta$  is the angle of reflection from the substrate- thin film interface,  $v_s$  is the sound velocity of the in the substrate and  $\lambda_{pr}$  represents the wavelength of the probe light. From equation (3.4) it is obvious that it is possible to determine the sound velocity within the material by detecting the oscillation period  $T$  of the relative reflective change at a certain probe wavelength as previously proposed in the literature<sup>9</sup>. Furthermore it also becomes clear that the oscillation period depends on the probe wavelength. The same equation can also be derived in the picture of the stimulated Brillouin backscattering condition where the phonon wavevector  $k_p$  leads to a change in the photon k-vector from  $+k_L$  to  $-k_L$ :

$$k_p = 2k_L = \frac{4\pi n}{\lambda_{pr}} \cos(\beta) \quad (3.5)$$

Since we examine phonons located in the center of the Brillouin zone, where the dispersion relation for acoustical phonons is linear one obtains:

$$v_s = \frac{\omega_p}{k_p} = \frac{\omega_p \lambda_{pr}}{4\pi n \cos(\beta)} \quad (3.6)$$

which after substituting  $\omega_p = 2\pi\nu$  yields the same result as the Bragg condition<sup>20</sup>. Relation 3.4 quantitatively discusses the occurrence of relative reflectivity oscillations that have been reported in the literature<sup>9</sup> on samples containing a metal transducers on  $\text{SiO}_2/\text{Si}$  substrates. In the following experiments I examine the strain pattern triggered by the trans-cis isomerization process of azobenzene and compare its phase to expanding thin films.

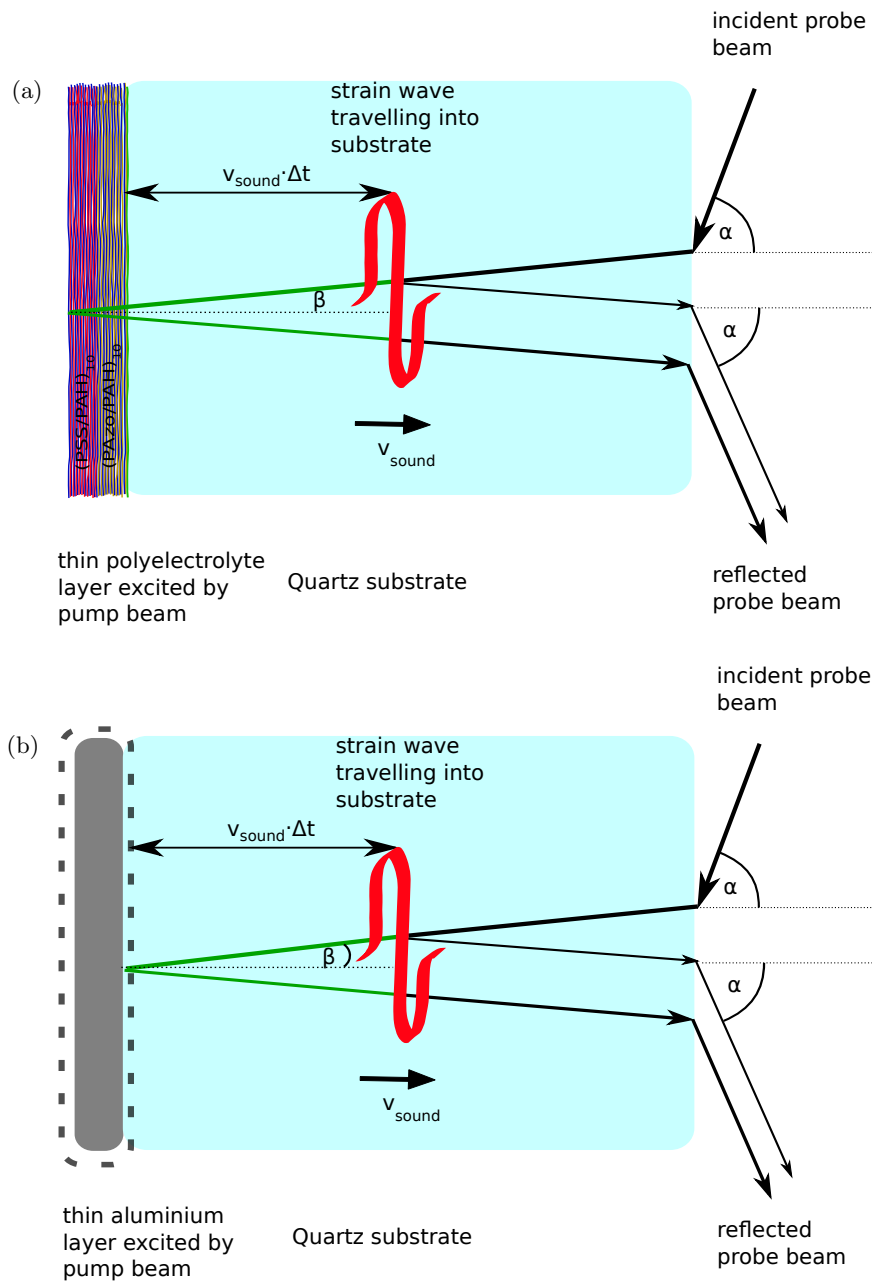


**Figure 3.7:** Schematic of the interference geometry for the relevant reflections of the probe beam (a) for the polyelectrolyte matrix containing 10 double layers (PAzo/PAH) as well as the Gold-nanoparticle-polyelectrolyte composite on the quartz substrate and (b) the 30 nm aluminium film, respectively. The differences in the optical path lengths relevant for the interference process have been colored green. The dominant reflection in (a) takes place at the polyelectrolyte/air interface with a relative reflection intensity of approximately 0.4 that is large compared to the relative reflection intensity of approximately 0.04 at the substrate-layer interface. For the thin aluminium layer approximately 80% of the incoming intensity is reflected at the quartz aluminium interface (b). The reflection intensities are estimated upon calculations using the Fresnel equations stated in section 3.3.2. The strain pulses are generated by the excitation of the azobenzene molecules within the thin polyelectrolyte film, by the expansion of the 10 nm gold-nanoparticles (a) or by the expansion of the thin aluminium layer (b).

### 3.3.2 Measurement and signal analysis of reflectivity change

Using the reflection geometry of the setup described in 3.1 I measured the relative reflectivity change in the previously prepared PAzo samples as well the Al and Au-nanoparticle samples. For the excitation of the PAzo samples I used the second harmonic of the Ti:Sa laser as pump beam that has a central wavelength of  $\lambda = 397.5$  nm because it is well in the range of the absorption peak depicted in figure 2.3(a) and thus is expected to induce changes within the polyelectrolyte. The maximum pump fluence of  $\Phi = 35 \frac{\text{mJ}}{\text{cm}^2}$  has been used because it induced the strongest signal. The data of the reflectivity change I obtained from the PAzo2 sample is depicted in 3.8. For this graphic the static background has been subtracted from the measured pump and probe signal but the relative reflectivity change signal is otherwise unchanged.

In order to minimize the influence of noise I averaged the first delay loops of three measurements on different spots of the sample because after the first delay loop a decrease of the reflection change could be observed, which indicates an onset of degradation.

Because the maximum change in the sample is induced at the best temporal overlap between pump and probe beam I could thereby identify the instant of zero delay within my measurements for each wavelength with sufficient accuracy. Due to dispersion of the white light used as probe beam this moment is different for each wavelength. That induces an offset within the delay between different wavelengths. To correct this dispersion the measured data for each wavelength has been shifted by an offset as already described for the transmission measurements in section 3.2.

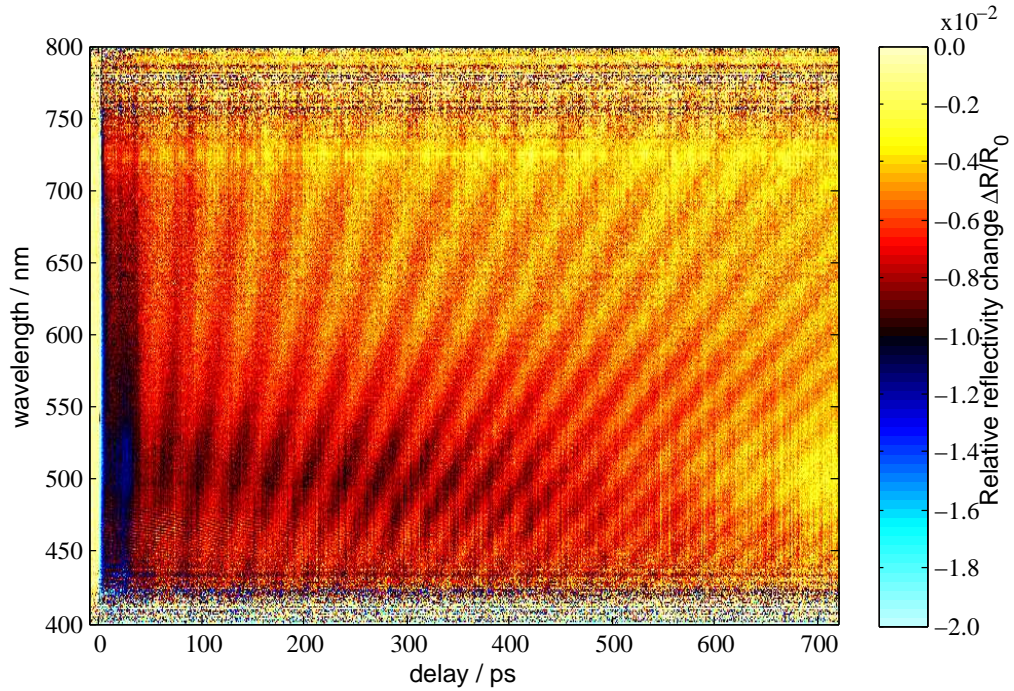


**Figure 3.8:** Relative reflectivity change  $\frac{\Delta R}{R_0}$  measured on 10 double layers of (PAzo/PAH) on quartz substrate with  $\lambda_{\text{pump}} = 397.5$  nm and a pump fluence of  $35 \frac{\text{mJ}}{\text{cm}^2}$ . One can see a strong change in the relative reflectivity at zero delay and a gradual decay over time, which is superimposed by a fanlike structure as predicted in section 3.3.1

The data presented in figure 3.8 already show pronounced oscillations in the detected reflectivity signal. It can be seen that the period of these oscillations continuously increases

with the wavelength making the image appear like a fan. In addition a strong peak in the reflectivity change can be seen at time zero. In order to better resolve the oscillatory component and to extract phase information I applied a signal analysis routine to the measurement. The steps of this routine are presented exemplarily for the response of the PAzo2 thin polyelectrolyte film.

At first I filtered the slowly varying components out of the oscillations by subtracting the running average over 200 ps from the data for each wavelength. Furthermore I cut the signal at a delay of 10 ps and thereby eliminate the fast dynamic component that is induced by the temporal overlap at zero delay. The result of this preliminary high pass filter is shown in figure 3.9.

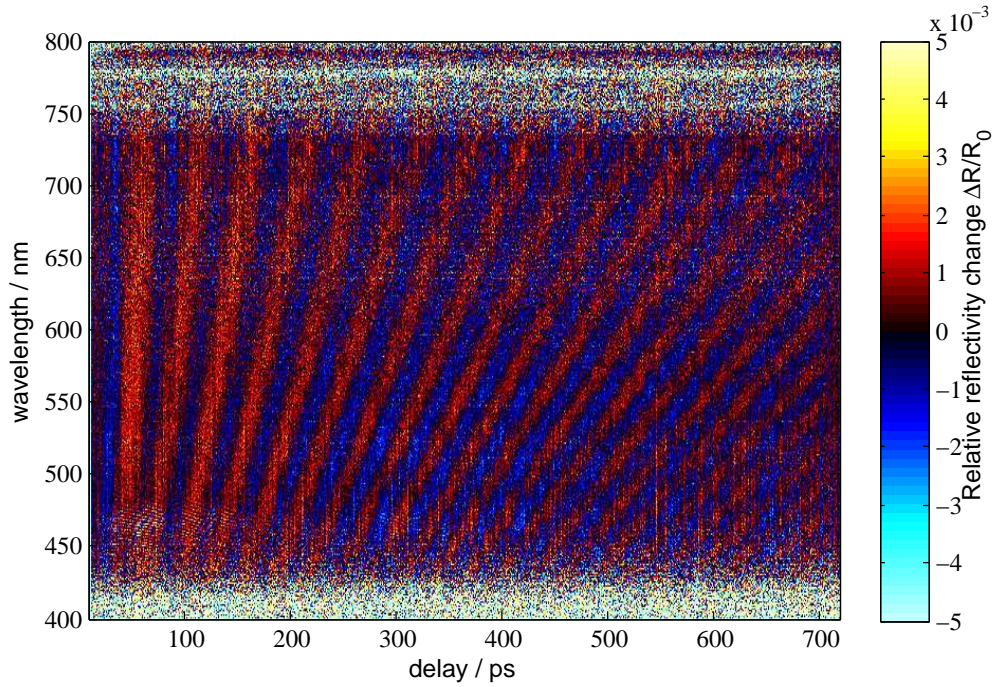


**Figure 3.9:** Oscillatory component of the relative reflectivity change data presented in figure 3.8 that has been extracted by subtraction of the slowly varying components from the signal as well as clipping of the strong change at time zero

In the next step a Gaussian bandpass filter has been used in order to filter the most prominent oscillation frequencies. For that I applied a Fast Fourier Transformation (FFT) to each probe wavelength line of the obtained oscillations from figure 3.9 in time and received a frequency spectrum with the amplitude of the oscillations depicted in 3.10(a). One can see a curved trend of the maximum amplitude within the frequency spectrum from approximately  $0.02 \text{ ps}^{-1}$  frequency at a wavelength of 750 nm increasing to approximately  $0.035 \text{ ps}^{-1}$  at a wavelength of 450 nm. This curve of the maximum oscillation amplitude corresponds to the dominant oscillations visible in figure 3.9.

In the next step I fitted the maximum of the absolute value of the Fast-Fourier transformation over the wavelength with a second order polynomial to determine the frequency around which I want to center the following bandpass. As a bandpass I used a Gaussian function with a FWHM of 20 data points, which correspond to a frequency range of  $0.071 \text{ ps}^{-1}$ . Figure 3.10(b) displays the FFT of the reflectivity oscillations after multiplying the amplitude for each wavelength with the Gaussian weight function. There one can see that the curve with maximum amplitude is successfully extracted while other frequencies

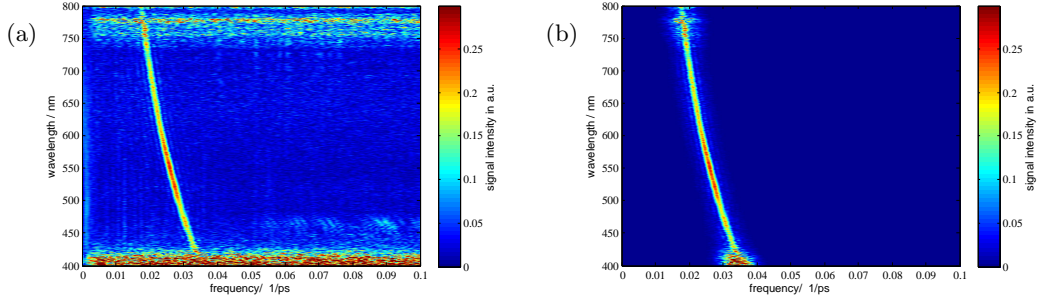


**Figure 3.10:** Fast Fourier Transformation of the relative reflectivity change oscillations measured on a sample containing 10 double layers of (PAzo/PAH) (a). A Gaussian weight function centred around the fit to the maximum amplitude at each wavelength is applied in order to damp the unwanted noise in the data (b). Both graphs show that the frequency with the highest amplitude varies from approximately  $0.02 \text{ ps}^{-1}$  at a probe wavelength of 750 nm to  $0.035 \text{ ps}^{-1}$  at a probe wavelength of 450 nm. This corresponds to an oscillation frequency in between 20 – 35 GHz.

that mainly correspond to noise in the measured data are damped. An inverse FFT of the data depicted in figure 3.11 consequently shows only the oscillations I wanted to extract from the original measurement in figure 3.8.

For reference purposes I also measured these Brillouin oscillations generated by a thin metal layer and the gold-nanoparticle polyelectrolyte composite material on top of the same quartz substrate. It is evident that a thin metal expands upon excitation of the sample and the expansion of the gold-nanoparticle-polyelectrolyte samples has been studied in our group<sup>11</sup>. In case that thin films of comparable thickness and with similar refractive indices are attached to identical substrates the phase of the relative reflectivity oscillations provides information about the expansion behavior of the thin films<sup>8</sup>. When the oscillations of the two samples are in phase under these circumstances they exhibit the same expansion behavior. Deviations in the thickness of thin films and remarkable differences in their complex indices of refraction lead to phase shifts in the observed reflectivity change that can be corrected as described later in equation (3.10). Consequently we have in principle an experimental method at hand that enables us to determine whether azobenzene is expanding or contracting upon excitation.

The obtained results from the gold nano-particle polyelectrolyte composite and the 30 nm thin aluminium film on a quartz substrate are assembled in figure 3.12(a)-(h). The aluminium layer sample has been excited with the fundamental wavelength of the Ti:Sa laser at 795 nm whereas the gold-nanoparticle-polyelectrolyte composite has been pumped by pulses with a central wavelength of 520 nm. These pulses with a wavelength close to the absorption of the composite material have been created by a Noncollinear Optical Parametric Amplifier (NOPA) setup.

The reflectivity change measured on the gold nano-particles at the left hand side of figure 3.12 shows a discontinuity at a wavelength of approximately 533 nm that can be observed at each stage of the signal analysis. The proximity to the used pump wavelength suggests me that the discontinuity is a pump related feature. On the other hand the discontinuity could also be due to the plasmonic resonance of the gold nanoparticles that falls in this spectral region. Kiel et al. have previously discussed the plasmonic resonance of the Au nanoparticles in the effective medium of the polymermatrix<sup>12</sup> and even experimentally determined the corresponding dielectric function  $\epsilon(\omega, t) = \epsilon(\omega, t)_r + i\epsilon(\omega, t)_i$ <sup>10</sup>. We know

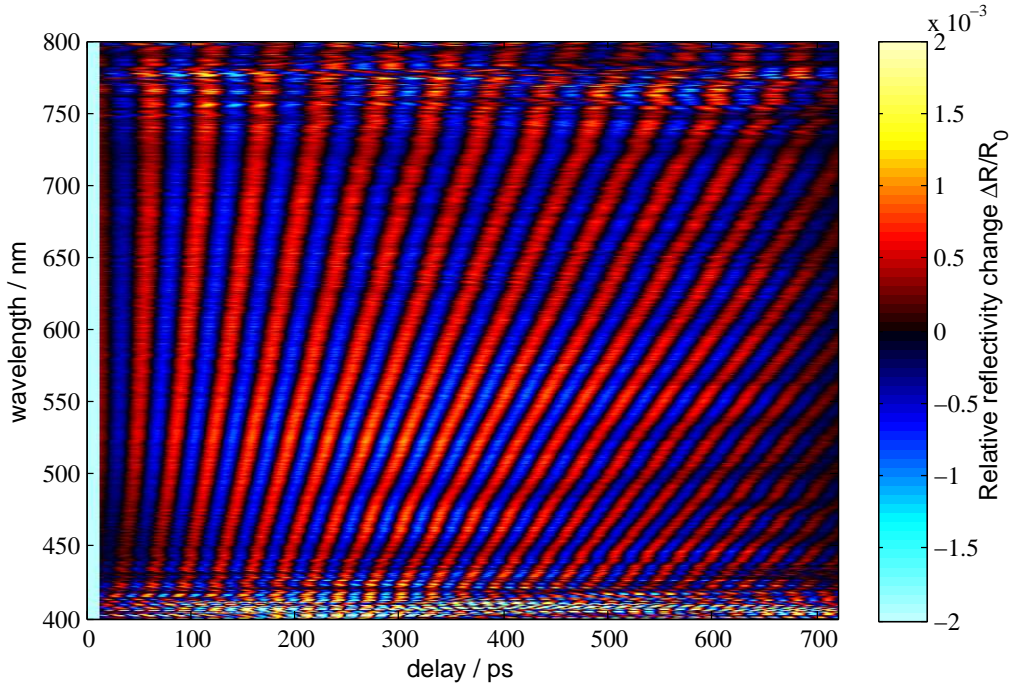


**Figure 3.11:** Inverse FFT of the smoothed signal presented in figure 3.9(b) that shows the final stage of the extraction process of the relative reflectivity oscillations measured on APAzo2. This is the data that is further used for comparison of the Brillouin oscillation phase with reference samples having a gold nanoparticle polymer composite or aluminium on top of the same quartz substrate.

that the imaginary part of the dielectric function has a maximum at the plasmonic resonance. As a consequence of the Kramers-Kronig relations between  $\epsilon_i(\omega)$  and  $\epsilon_r(\omega)$  we expect not only to see a change in transmittance  $\Delta T(\omega)$ , which qualitatively corresponds to  $\Delta\epsilon_i(\omega)$  but also a change in reflectivity  $\Delta R(\omega)$  that qualitatively corresponds to  $\Delta\epsilon_r(\omega)$ . Repeating the measurement for the same gold-polyelectrolyte composite at a different pump wavelength would enable us to decide, which of these two processes is dominant. If the discontinuity shifts with the used pump wavelength it is most likely an artefact and if its spectral position is preserved then it could be an interesting feature of the plasmonic effect that could be studied further.

To omit these complications for now I limit myself to compare the oscillation phase between Au-nanoparticles and the PAzo sample at a wavelength of 700 – 750 nm, which is in a spectral region well above the plasmonic resonance and the pump wavelength. The comparison of the oscillations between the azobenzene and gold nanoparticle sample is displayed in 3.12(a). It shows that the oscillations are well in phase in the spectral region between 700 – 750 nm. Furthermore we also measured the relative reflectivity change in a thin aluminium film sample, which serves as a second reference that does not have a plasmonic feature in the visible range. The obtained data is presented in 3.12(b). The relative reflectivity oscillations of the PAzo and the thin aluminium film sample appear to have a phase shift close to 180° over the entire spectrum.

To extract the information about the behaviour of azobenzene upon excitation from the phase of the relative reflectivity oscillations one has to consider the different contributions to the phase. The detected signal intensity originates from an interference of two electromagnetic waves, the reflection at the strain pulse  $E_1$  and the dominant reflection at

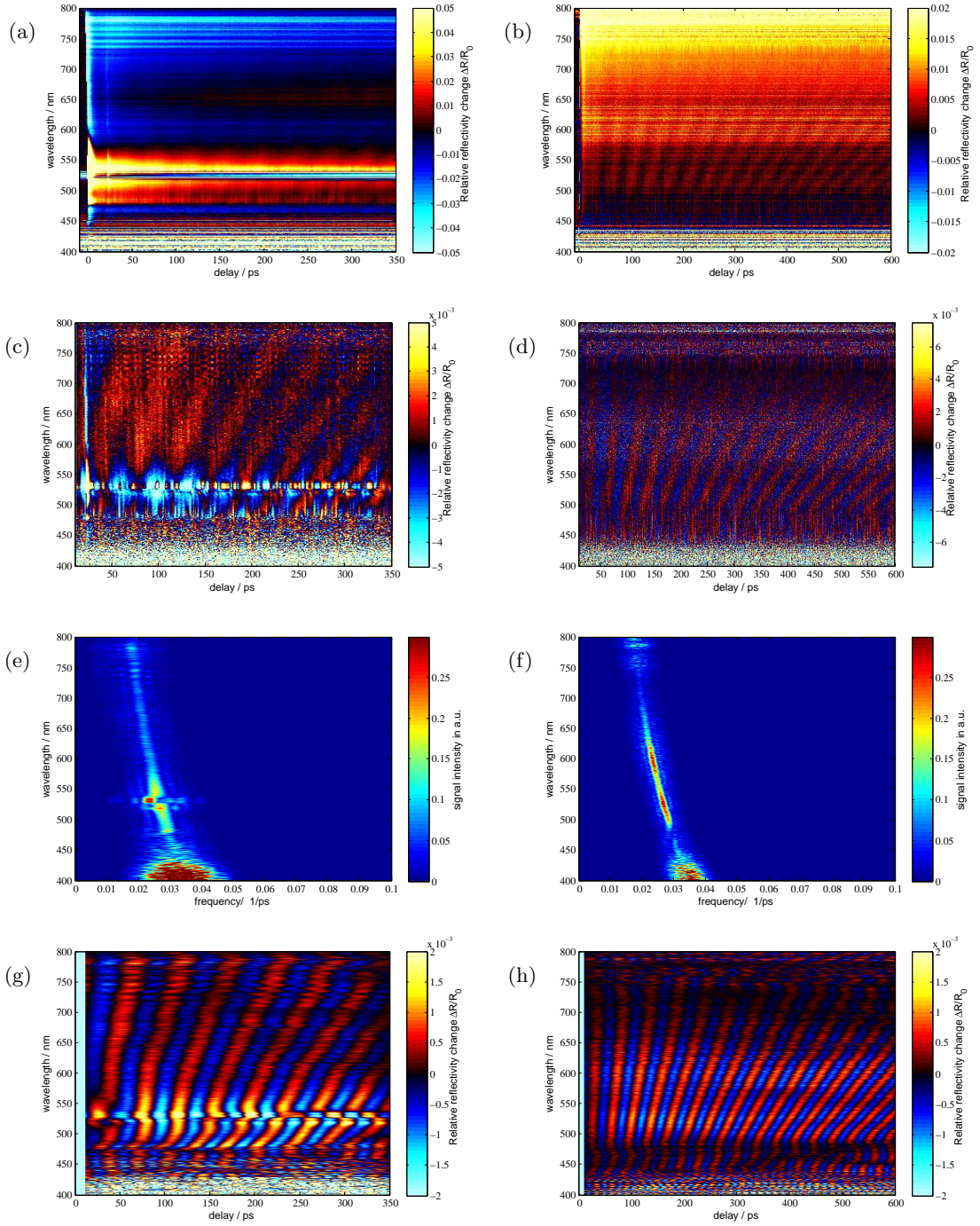


**Figure 3.12:** Signal analysis steps from the measured relative reflectivity change to the extracted Brillouin oscillations in the reference samples. Pictures on the left hand side show the measured response of the AAu sample as compared to the results of the AAl sample on the right side. The measured relative reflectivity change of the gold-nanoparticle-polyelectrolyte composite from (a) is cut at delay time of 10 ps and submitted to a highpass filter to extract the high frequency components oscillations displayed in (c). Via a Fast Fourier Transformation of (c) one obtains the amplitude of the of different oscillations frequencies that are weighted with a gaussian filter (e). The inverse Fourier Transformation then yields the relevant oscillations with reduced noise. The same steps are applied to the relative reflectivity oscillations of the thin aluminium film in (b),(d),(f),(h). Note that the measured signals qualitatively resemble each other apart from the discontinuity in the AAu sample at the wavelength of approximately 533 nm that requires further measurements in order to determine its origin.

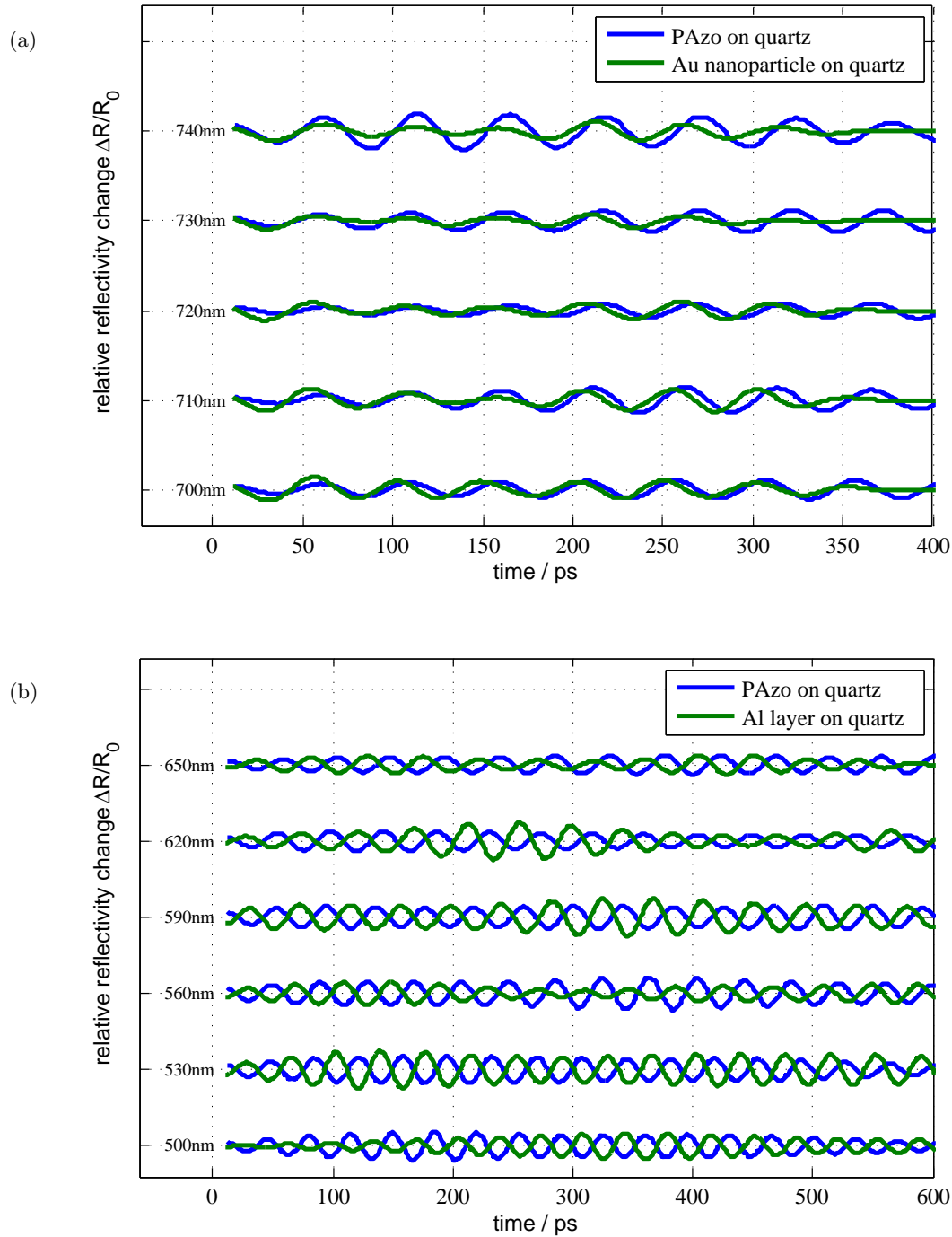


**Figure 3.13:** (a): Comparison of wavelength slices through the relative reflectivity oscillation signal between PAzo in a polymer matrix extracted from figure 3.11 and the gold-nanoparticle-polyelectrolyte composite extracted from figure 3.12(g). The oscillations are compared in a spectral region distant to the plasmonic resonance of gold nanoparticles. The oscillations are rather in phase. (b): Comparison of the oscillations between the PAzo sample and a 30 nm aluminium film extracted from figure 3.12(h). The oscillations have a relative phase of approximately 180°. To correctly relate the measured phase to an expansion behavior one has to calculate the phase shifts that the electromagnetic wave undergoes at each interface and due to different optical path lengths in the thin films. A definite conclusion from these experimental findings requires the knowledge of the complex refractive index for the involved thin films and their exact thickness that is needed in order to calculate the phase shifts at the interfaces and the contribution by the additional propagation time in the medium.

the thin film  $E_2$ , as it is depicted in figure 3.7. The intensity at the spectrometer  $I(\Delta t)$  consequently depends on the relative phase  $\Delta\phi$  between the two electromagnetic waves as it is derived in equation (3.8).

$$I(\Delta t) \propto |E_1 + E_2|^2 = |E_1|^2 + 2E_1 \cdot E_2 + |E_2|^2 \quad (3.7)$$

$$= |E_1|^2 + 2|E_1|^2|E_2|^2\cos(\Delta\phi) + |E_2|^2 \quad (3.8)$$

Since the measurement routine determines the relative reflection change between the sample in the pumped and unpumped state the static reflection intensity  $|E_1|^2$  does not contribute to the signal. The induced change in the refractive index by the strain pulse is relatively small. Therefore the term  $|E_2|^2$  is a minor contribution to the detected signal intensity  $I(\Delta t)$ . Consequently the dominant contribution to the signal is the interference term  $2|E_1|^2|E_2|^2\cos(\Delta\phi)$ . The contributions to the relative phase  $\Delta\phi$  are summarized in equation 3.10. Since the oscillation frequency  $\omega$  and the wave vector  $k$  are the same for both electromagnetic waves  $E_1$  and  $E_2$  their contribution to relative phase cancel each other out. Hence  $\Delta\phi$  only consists of the various phase shifts upon transmission and reflection as well as the difference in the optical path lengths between  $E_1$  and  $E_2$ . The terms that appear in equation (3.10) are discussed exemplarily for the reflection at the APAzo2 azobenzene-polyelectrolyte thin film sample.

$$\Delta\phi = \phi_2 - \phi_1 \quad (3.9)$$

$$= \underbrace{\arg(t_{qf}r_{fv}t_{fq})}_{\substack{E_2 \text{ phase shift} \\ \text{at interfaces}}} - \underbrace{\frac{4\pi n_f d_f \cos(\alpha)}{\lambda}}_{\substack{E_2 \text{ phase shift in} \\ \text{thin film}}} - \underbrace{\frac{4\pi n_q v_q \Delta t \cos(\alpha)}{\lambda}}_{\substack{E_2 \text{ phase shift in} \\ \text{substrate}}} - \underbrace{\Delta\phi_{r_{sp}}}_{\substack{E_1 \text{ phase shift} \\ \text{at strain pulse}}} \quad (3.10)$$

### Phase shift at the interfaces

The reflection and transmission of the used s-polarized probe light at an interface is described by the Fresnel equations (3.11) and (3.12). In the used version of the Fresnel equations we assumed that the magnetic contributions are negligible in all our media and therefore set the relative magnetic permeabilities of the media  $\mu_{r1} = \mu_{r2} = 1$ .

$$t_s = \left( \frac{E_{0t}}{E_{0e}} \right)_s = \frac{2N_1 \cos \alpha}{N_1 \cos \alpha + N_2 \cos \beta} = \frac{2N_1 \cos \alpha}{N_1 \cos \alpha + \sqrt{N_2^2 - N_1^2 \sin^2 \alpha}} \quad (3.11)$$

$$r_s = \left( \frac{E_{0r}}{E_{0i}} \right)_s = \frac{N_1 \cos \alpha - N_2 \cos \beta}{N_1 \cos \alpha + N_2 \cos \beta} = \frac{N_1 \cos \alpha - \sqrt{N_2^2 - N_1^2 \sin^2 \alpha}}{N_1 \cos \alpha + \sqrt{N_2^2 - N_1^2 \sin^2 \alpha}} \quad (3.12)$$

Thus the reflection coefficient  $r_s$  as well as the transmission coefficient  $t_s$  can be computed if the complex refractive index  $N = n + i\kappa$  of the first and the second medium as well as the angle of incidence  $\alpha$  relative to the perpendicular are known. The polar angle of the complex coefficients  $r_s$  and  $t_s$  in the complex plane then determines the phase shift the electromagnetic wave experiences upon reflection respectively transmission at the interface. In equation (3.10)  $t_{qf}$  represents the transmission coefficient from the quartz substrate to the thin film,  $r_{fv}$  stands for the reflection coefficient at the substrate air interface and  $t_{fq}$  is the transmission coefficient at the thin film quartz interface.

The reflected light intensity at an interface is proportional to  $|r|^2$ , so that we have a way to determine if the interference condition is dominated by the static reflection at the substrate thin film interface  $|r_{qf}|^2$  or the reflection at the thin film air interface  $|r_{fv}|^2$ . The

refractive index of the polyelectrolyte-azobenzene composite is assumed to be close to the refractive index of the gold-nanoparticle-polyelectrolyte composite ( $n = 1.58$ )<sup>12</sup>, which in turn is close to the refractive index of the quartz disc ( $n = 1.45$ )<sup>21</sup>. Using these values as approximations I obtained  $|r_{qf}|^2 \leq 8\%$  whereas  $|r_{fv}|^2 \geq 40\%$  so that the relevant reflection takes place at the thin film air interface. On the contrary using the refractive indices for aluminium from the literature<sup>22</sup> I calculated that the relevant reflection in this case takes place at the substrate aluminium interface  $|r_{qf}|^2 \approx 80\%$ . That justifies the two different beam geometries depicted in figure 3.7, which also implies a different interface contribution  $\arg(r_{qf})$  for the aluminium layer.

### Phase shift due to differences in the optical pathlengths

Figure 3.7 illustrates that the electromagnetic wave  $E_2$  reflected from the substrate has to travel a longer optical path as the electromagnetic wave reflected as the strain pulse. The additional phase shift induced by the propagation time of the electromagnetic wave between two parallel surfaces  $\Delta\phi_{\text{prop}}$  is stated in equation (3.13) as derived in optic textbooks<sup>23</sup>.

$$\Delta\phi_{\text{prop}} = -\frac{4\pi nd}{\lambda} \cos(\alpha) \quad (3.13)$$

In equation (3.13)  $\alpha$  is again the angle of incidence relative to the perpendicular,  $\lambda$  is the considered probe light wavelength,  $n$  represents the real part of the refractive index and  $d$  the thickness of the medium in which the electromagnetic wave has to travel an additional optical path. That sufficiently describes the static phase shift of  $E_2$  due to the propagation in a thin film that has to be taken into consideration for the polyelectrolyte materials. The phase shift due to the propagation in the substrate can be described by the same equation with the modification that the additional optical path length is time dependent  $d = v_q \Delta t$  since the strain pulse travels at the speed of sound of the substrate  $v_q$ .

### Phase shift at the strain pulse

The phase shift of  $E_1$  upon reflection at the strain pulse  $\Delta\phi_{r_{sp}}$  has been analyzed in the literature<sup>8</sup>. There one can see that the phase shift depends on the shape of the strain pulse. If the thin film is expanding upon excitation with the laser pulse the compressive part of the bipolar strain pulse precedes the tensile part and vice versa in case that the thin layer is contracting upon excitation. An inversion of the strain pattern from an expanding to a contracting thin film, that leaves the shape of the strain pattern otherwise unchanged, would lead to a relative phase shift of  $180^\circ$  in  $\Delta\phi_{r_{sp}}$ .

If we correct the phase of the Brillouin oscillations by the contributions from the phase shifts due to the reflections at interfaces and the additional optical path lengths the phase shift due to the reflection at the strain pulse is the only remaining unknown. Therefore we can obtain an information about the expansion or compression of the medium. If for example the corrected Brillouin oscillations of the azobenzene-polyelectrolyte thin film and the Brillouin oscillations triggered by the expanding thin aluminium film are in phase we can conclude that the azobenzene thin film is also expanding. If we observe a relative phase in the corrected oscillations of  $180^\circ$  then we would conclude that the azobenzene thin film is contracting upon ultrafast excitation.

At this point of the experiments we do not know the complex refractive index of the used materials well enough to conduct the necessary corrections in the phase. The theoretical background necessary for further investigations has been prepared so that the expansion behavior of the azobenzene polyelectrolyte thin films can be identified in the future. The complex refractive index of the transparent thin film samples can be determined via

---

transmission and reflection measurements. The complex index of refraction of the relatively nontransparent aluminium thin film could be measured via white light ellipsometry.

## 4 Conclusion

### 4.1 Summary of the results

With the conducted experiments I investigated the trans-cis isomerization of azobenzene in thin polyelectrolyte films, that have been prepared via spin assisted layer-by-layer deposition. The used preparation technique successfully incorporated azobenzene into the polyelectrolytes, which led to a characteristic minimum in the transmission spectrum at 365 nm that I assigned to the  $\pi\pi_{trans}^*$ -transition of the energetic ground state. The redshift of the transition band relative to the 315 nm observed for  $\pi\pi_{trans}^*$ -transition in hexane solution<sup>5</sup> and the 330 nm observed in ethanol solution<sup>2</sup> is consistent with a solvatochromism that becomes larger with increasing polarity of the surroundings. My findings are also consistent with the results published for comparable azobenzene polyelectrolyte thin films where the absorption has been found at 360 nm and the possibility of reversible photoinduced switching has been shown<sup>15</sup>. In agreement with the literature I noted that the absorption assigned to the azobenzene trans-state decreases after resonant irradiation at 365 nm that partially isomerizes some molecules to the cis-state. I observed a recovery of the absorption either by irradiation in the visible part of the spectrum or via thermal processes occurring over time.

I primarily investigated the reaction dynamics with ultrafast pump-probe-spectroscopy and noted a transient absorption upon excitation with 400 nm pump pulses that is present in the visible range and has its maximum intensity within the wavelength interval of 450 – 650 nm. The transient absorption is observed to decay with a time constant of approximately  $5 \pm 1$  ps. At this stage of the analysis it is not consistent with the decay constants  $\tau_1 \leq 0.2$  ps,  $\tau_2 \approx 0.9$  ps and  $\tau_3 \approx 15$  ps that are reported in the literature for experiments on trans-azobenzene in solution<sup>5</sup>. Nevertheless a similar time scale has been observed on azobenzene incorporated into functionalized polymer colloids<sup>19</sup> at the group of Prof. Temps at the university in Kiel.

The analysis of the mono-exponential fits indicated a constant offset persistent for delays greater than 15 ps that we noted to decay within 60 ps. We tentatively conclude that the polyelectrolyte surrounding severely influences the potential energy landscape depicted in figure 1.2 so that a different decay process is altered for azobenzene in a polyelectrolyte matrix. Our first guess is that the dense packing and the strong interaction of the azobenzene with the neighbouring polymer decreases the speed of its reaction dynamics due to steric hindrance effects.

In the final experiments I demonstrated that the excitation of the azobenzene molecules is able to trigger a strain pulse with dominant GHz frequency components similar to the processes that are reported in the literature for metal transducers<sup>9</sup>. The existence of the Brillouin oscillations that I detected via pump-probe-spectroscopy indicates a reversible process that triggers the strain pulse. Because a complete trans-cis isomerization of the azobenzene molecules would diminish their absorption at the used pump wavelength of 400 nm, we conclude that the dynamics leading to the induced strain wave should have a different origin. We tentatively suggest that the polyelectrolytes that are strongly bound to

their counter ions respond to the excitation via an onset of the isomerization movement but the electrostatic interactions force them back into the trans-configuration so that they are available for the next excitation. Combining the fact that the layers are highly stratified due to the preparation routine and this tentative explanation we developed a schematic picture of the alignment of the azobenzene containing side chains of the polyelectrolyte thin film. Our proposition is depicted in figure 4.1. We propose that the charged side groups in the PAH/PAzo layers that contain the azobenzene point away from the polymer backbone and are rather aligned to point to the polyelectrolyte counter ion of the opposite layer. Nevertheless the distance and thus the strength of the bonds varies within the electrolyte groups.

The comparison of the phase of the stimulated Brillouin oscillations between the excited azobenzene and a thin aluminium layer as well as a gold-nanoparticle polyelectrolyte composite indicates an expansion of the polyelectrolyte film containing the PAzo layers. We noted that the amplitude of the detected Brillouin oscillations from the azobenzene-polyelectrolyte-composite is comparable with the amplitude from the reference samples, making azobenzene a promising molecule for further studies on its mechanical response induced by photo-isomerization.

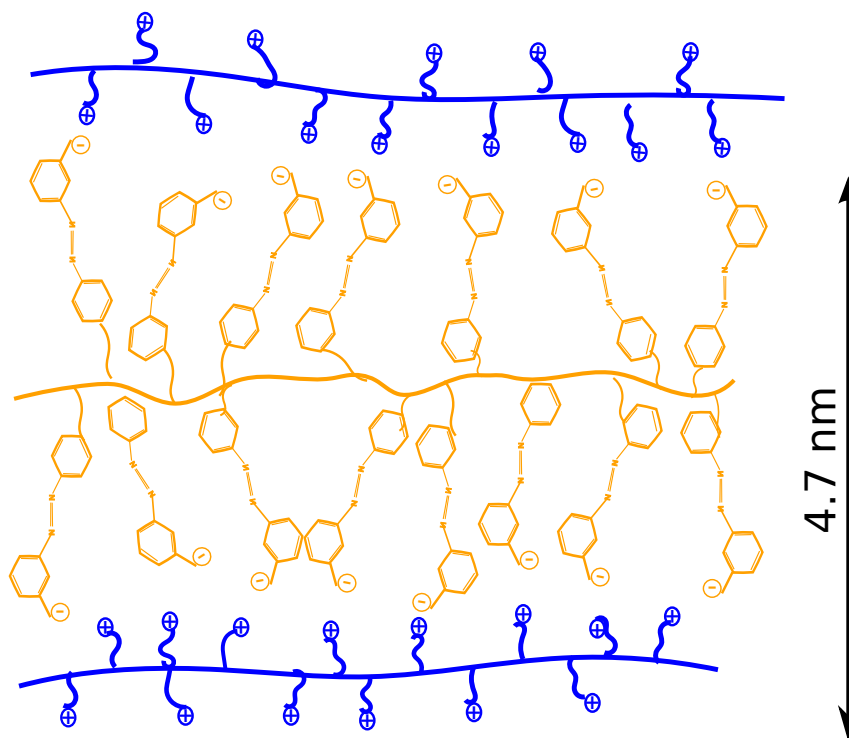


**Figure 4.1:** Schematic of the suggested alignment of the PAzo molecules in the polyelectrolyte thin films. The azobenzene molecules are aligned due to electrostatic repulsion from each other and attraction to their counter ions located at the opposite polyelectrolyte. The distance between the charged groups varies, leaving some azobenzene molecules relatively weakly bonded, whereas others are expected to be strongly bound.

## 4.2 Outlook on further experiments

The results of my experiments with azobenzene in polyelectrolyte thin films provide a basic understanding of the properties and dynamics of the prepared system but they also spark

new questions and ideas for possible further experiments based on the progress made so far. Currently additional experiments concerning the steady state transmission spectroscopy that use a 300 W mercury-vapor lamp and optical filters that allow for alternate irradiation in the UV-spectrum at  $\lambda < 340$  nm and in the visible range of the spectrum at  $\lambda > 450$  nm are in progress. Their aim is to elaborate on the directed switching between the cis- and trans-configuration and investigate the saturation limit for the photoinduced isomerization process. Furthermore it is desirable to detect the  $n\pi^*$  as well as the  $\pi\pi^*_{cis}$  characteristic absorption for the prepared samples that have not been assigned due to the relatively small extinction coefficient of the  $n\pi^*$ -transition and the spectral overlap between the  $\pi\pi^*_{trans}$ - and  $\pi\pi^*_{cis}$  band. We expect to identify them in the case that a higher cis population can be prepared via longer irradiation in the UV spectrum at a higher intensity. We are also working on polarization dependent transition spectroscopy measurements to test the hypothesis that the majority of the azobenzene groups are aligned perpendicular to the surface layer as suggested in figure 4.1. Accordingly the dipole moments would also be oriented perpendicular to the surface leading to a higher extinction for p-polarized light than for s-polarized light at an angle of incidence of  $45^\circ$ .

The next step for the time resolved transient absorption pump-probe spectroscopy is the usage of other substrates that are transparent over a comparably range of the UV-Vis spectrum as the employed quartz discs but exhibit less artefacts due to the non-linear interactions at zero delay. That would enable us to better resolve the ultrafast processes at delay times smaller than 0.5 ps where even faster dynamics could occur. Furthermore it would be interesting to study a systematic variation of the used pump wavelength using the available NOPA system. Thereby we can readily tune the wavelength in the visible range and via second harmonic generation in a nonlinear crystal the NOPA also permits to pump in the UV spectrum. It would be interesting to know if the signal intensity significantly increases or reveals even different characteristics when the sample is pumped at the resonance wavelength  $\lambda_{\pi\pi^*trans} = 365$  nm or at the resonance of the fundamental  $\lambda_{n\pi^*trans}$ -transition that is expected<sup>17</sup> at approximately 445 nm. An increased relative transmittance change could be used to verify the existence of the second decay process via a double exponential fit on newly measured data based on the scheme presented in section 3.2. In addition possible two photon processes could be identified if a pump fluence dependence of the sample response is investigated.

A further study of the very promising stimulated Brillouin backscattering experiments presented in section 3.3 is aspired. Using samples with a known complex index of refraction or determining the properties of the used samples would enable us to determine the expansion behavior of azobenzene in polyelectrolyte thin films. At this point of the experiments we can not come forward with a definite statement, whether the azobenzene polyelectrolyte thin film is expanding or contraction upon irradiation. Nevertheless the necessary future analysis steps have been presented in section 3.3.2.

With regards to possible applications of azobenzene polyelectrolyte thin films as a transducer it would be very interesting to know how one can manipulate the amplitude of induced strain pattern that is proportional to the amplitude of the Brillouin oscillations. Therefore fluence dependent measurements of the signal amplitude is a next step towards a more complete understanding of isomerization processes in this particular surrounding. Furthermore it is necessary to understand how much of the signal amplitude can be attributed to the trans-cis isomerization of the azobenzene units and how large the contribution of thermal expansion is in that process. That can be achieved by replacing the azobenzene

group in the polyelectrolyte by another chromophore unit such as rhodamine that does not exhibit any photochromism but at least partially absorbs the incident pump light leading to thermal excitation of the thin layer.

Yet to gain a throughout understanding of the sample properties it is desirable to expand the experimental techniques beyond the optical pump-probe spectroscopy described here. Using a streak camera as detection device I also constructed a setup that allows for time resolved measurements of the fluorescence spectrum of liquid as well as thin film samples and did some preparatory measurements of the fluorescence spectrum of the azobenzene in thin polyelectrolyte films. By detecting the emitted light of a sample that is excited with femtosecond laser pulses the time resolved fluorescence measurement provides information on the decay channels of the excited state. Via Laser-induced Fluorescence (LiF) detected by a streak camera one can determine the relative intensities as well as the decay times of the detected transitions, which yields complementary information to the transient absorption spectroscopy where the excited state is probed via its absorptions. The natural next step for these experiments is to identify the fluorescence maxima and their decay times upon excitation at the pump wavelength of 400 nm that has been used as a pump wavelength in the experiments presented here. Then it is interesting to investigate the changes in the time resolved fluorescence spectrum when the excitation energy is adjusted from the  $\pi\pi^*$ - to the  $n\pi^*$ -transition so that it is possible to detect characteristic fluorescence features of the  $S_1$  as well as the  $S_2$  potential energy state. Even multiple excitations leading to higher energy levels as the  $S_2$  state of the thin polyelectrolyte films are possible. For example one could pump the sample to the  $S_2$ -state via a pump pulse at approximately 400 nm, probe the excited state with a second laser pulse to the overlying energetic level and detect the resulting fluorescence using the Streak camera as identifier. Thereby one can gain insight in dynamics that go beyond the theoretically predicted transitions presented in section 1.2. A long term goal of the transient absorption experiments as well as the Laser-induced fluorescence experiments is to assign decay constants to the excited states of the potential energy surfaces presented in figure 1.2 for azobenzene in polyelectrolyte thin films upon excitation of the  $n\pi^*$ - and the  $\pi\pi^*$ -transition.

At the end I present a so far speculative but interesting application that unifies the processes that I have investigated in this thesis. After having understood the details of each sub-process it would be interesting to build samples of layered polyelectrolytes that have azobenzene molecules incorporated at the one end that trigger a GHz-strain pulse upon excitation as investigated in section 3.3, which then would propagate through the polymer matrix. At the other end of the sample the strain pulse could trigger a new dynamic in functional groups that are sensitive to the strain. For example one could include fluorophores that change their fluorescence spectrum due to the compressive and tensile part of the strain pattern created at the other end of the polyelectrolyte layer. A schematic depiction of this speculative process is depicted in 4.2.

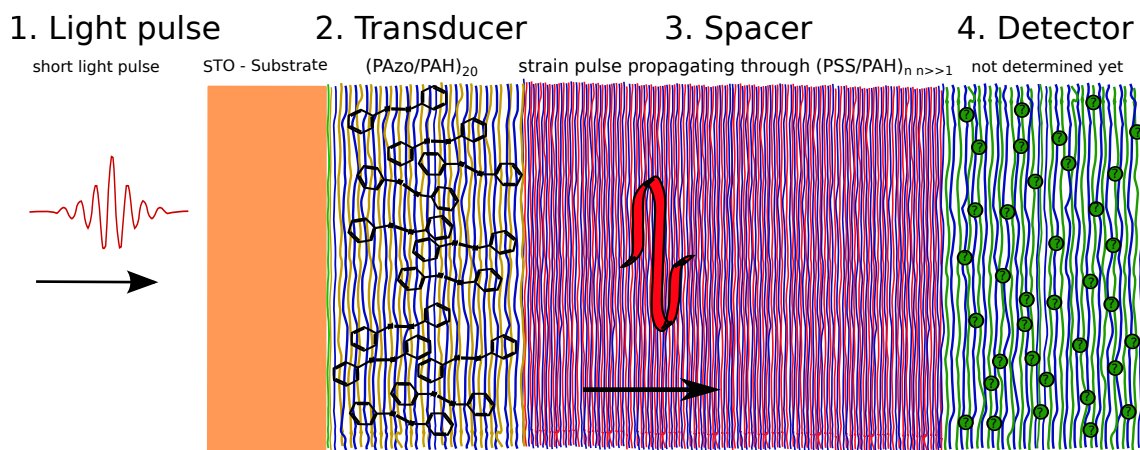


**Figure 4.2:** Schematic of a speculative application of the trans-cis isomerization and the related stimulated Brillouin backscattering process that have been investigated in this thesis. A short light pulse stimulates the azobenzene molecules incorporated into a polyelectrolyte thin layer. The isomerization process triggers a strain pulse that propagates into the adjacent spacer layers. When it reaches the strain sensitive molecules at the other end of the sample a change in their optical properties can be detected. A possible detection mechanism could be the change in the fluorescence spectrum of the detector molecules.

# Bibliography

- [1] N. Tamai and H. Miyasaka, “Ultrafast Dynamics of Photochromic Systems,” Chemical Reviews, vol. 100, no. 5, pp. 1875–1890, 2000.
- [2] N. T., H. R., W. Zinth, and J. Wachtveitl, “Femtosecond photoisomerization of cis-azobenzene,” Chemical Physics Letters, no. 272, pp. 489–495, 1997.
- [3] T. Ikeda and O. Tsutsumi, “Optical Switching and Image Storage by Means of Azobenzene Liquid-Crystal Films,” Science, vol. 268, no. 5219, pp. 1873–1875, 1995.
- [4] Z. Liu, K. Hashimoto, and A. Fujishima, “Photoelectrochemical information storage using an azobenzene derivative,” Nature, vol. 347, pp. 658–660, OCT 18 1990.
- [5] I. Lednev, T.-Q. Ye, P. Matousek, M. Towrie, P. Foggi, F. Neuwahl, S. Umaphathy, R. Hester, and J. Moore, “Femtosecond time-resolved UV-visible absorption spectroscopy of trans-azobenzene: dependence on excitation wavelength,” Chemical Physics Letters, vol. 290, no. 1–3, pp. 68–74, 1998.
- [6] S. Monti, G. Orlandi, and P. Palmieri, “Features of the photochemically active state surfaces of azobenzene,” Chemical Physics, vol. 71, no. 1, pp. 87–99, 1982.
- [7] M. Kiel, S. Mitzscherling, W. Leitenberger, S. Santer, B. Tiersch, T. K. Sievers, H. Möhwald, and M. Bargheer, “Structural Characterization of a Spin-Assisted Colloid-Polyelectrolyte Assembly: Stratified Multilayer Thin Films,” Langmuir, vol. 26, no. 23, pp. 18499–18502, 2010.
- [8] C. Thomsen, H. T. Grahn, H. J. Maris, and J. Tauc, “Surface generation and detection of phonons by picosecond light pulses,” Phys. Rev. B, vol. 34, pp. 4129–4138, Sep 1986.
- [9] E. Pontecorvo, M. Ortolani, D. Polli, M. Ferretti, G. Ruocco, G. Cerullo, and T. Scopigno, “Visualizing coherent phonon propagation in the 100 GHz range: A broadband picosecond acoustics approach,” Appl. Phys. Lett., vol. 98, no. 1, p. 011901, 2011.
- [10] M. Kiel, H. Möhwald, and M. Bargheer, “Broadband measurements of the transient optical complex dielectric function of a nanoparticle/polymer composite upon ultrafast excitation,” Phys. Rev. B, vol. 84, p. 165121, Oct 2011.
- [11] M. Kiel, Static and Ultrafast Optical Properties of Nanolayered Composites. PhD thesis, University of Potsdam, 07 2012.
- [12] M. Kiel, M. Klötzer, S. Mitzscherling, and M. Bargheer, “Measuring the Range of Plasmonic Interaction,” Langmuir, vol. 28, no. 10, pp. 4800–4804, 2012.
- [13] A. Marini, A. Munoz-Losa, A. Biancardi, and B. Mennucci, “What is Solvatochromism?,” The Journal of Physical Chemistry B, vol. 114, no. 51, pp. 17128–17135, 2010.

- [14] J. Bahrenburg, K. Rottger, R. Siewertsen, F. Renth, and F. Temps, “Sequential photoisomerisation dynamics of the push-pull azobenzene Disperse Red 1,” Photochem. Photobiol. Sci., vol. 11, pp. 1210–1219, 2012.
- [15] A. Toutianoush, F. Saremi, and B. Tieke, “Photoinduced switching in self-assembled multilayers of ionenes and bolaamphiphiles containing azobenzene units,” Materials Science and Engineering: C, vol. 8–9, no. 0, pp. 343–352, 1999.
- [16] A. Toutianoush and B. Tieke, “Photoinduced switching in self-assembled multilayers of azobenzene-containing ionene polycations and anionic polyelectrolytes,” Macromolecular Rapid Communications, vol. 19, no. 11, pp. 591–595, 1998.
- [17] F. Saremi and B. Tieke, “Photoinduced switching in self-assembled multilayers of an azobenzene bolaamphiphile and polyelectrolytes,” Advanced Materials, vol. 10, no. 5, pp. 388–391, 1998.
- [18] R. Menzel, Photonics: Linear And Nonlinear Interactions of Laser Light And Matter. Advanced Texts in Physics, Berlin, Heidelberg, New York: Springer, 2007.
- [19] J. Bahrenberg and F. Temps, “Private communication,” 2012.
- [20] A. Bojahr, M. Herzog, D. Schick, I. Vrejoiu, and M. Bargheer, “Calibrated real time detection of nonlinearly propagating strain waves,” submitted, 2012.
- [21] T. P. inc., “Technical Information about GE 124 Quartz Material,” July 2012.
- [22] A. D. Rakić, “Algorithm for the determination of intrinsic optical constants of metal films: application to aluminum,” Appl. Opt., vol. 34, pp. 4755–4767, 1995.
- [23] M. V. Klein and T. E. Furtak, Optik. Springer Berlin / Heidelberg, 1988.

# Statement of authorship

I hereby certify that this bachelor's thesis was written independently and without assistance from third parties. Other than the stated sources and aids were not used. Parts of the sources that have been used verbatim or in substance are identified as such. This bachelor thesis has not been presented in the same or similar form to any audit authority and it was not previously published elsewhere.

Hiermit versichere ich, dass die vorliegende Bachelorarbeit selbstständig und ohne Hilfe Dritter verfasst habe. Andere als die angegebenen Quellen und Hilfsmittel wurden nicht verwendet. Die den benutzten Quellen wörtlich oder inhaltlich entnommenen Abschnitte sind als solche kenntlich gemacht. Diese Bachelorarbeit hat in gleicher oder ähnlicher Form noch keiner Prüfungsbehörde vorgelegen und wurde auch nicht veröffentlicht.

Potsdam, 8.8.2012

(Alexander von Reppert)